TRIBHUVAN UNIVERSITY

INSTITUTE OF ENGINEERING

PULCHOWK CAMPUS

THESIS NO: 076/MSMSE/003

Fabrication of Metal Oxide/ Activated Carbon Nanocomposite from Jujube (Ziziphus Mauritiana) Seeds for Photodegradation of Dye

by

Anshu Kumari

A THESIS

SUBMITTED TO THE DEPARTMENT OF APPLIED SCIENCES AND CHEMICAL ENGINEERING IN PARTIAL FULFILLMENT OF THE REQUIREMENTS FOR THE DEGREE OF MASTER IN MATERIAL SCIENCE AND ENGINEERING

DEPARTMENT OF APPLIED SCIENCES AND CHEMICAL ENGINEERING

LALITPUR, NEPAL

OCTOBER, 2022

COPYRIGHT

APPROVAL PAGE

TRIBHUWAN UNIVERSITY

INSTITUTE OF ENGINEERING

PULCHOWK CAMPUS

DEPARTMENT OF APPLIED SCIENCES AND CHEMICAL ENGINEERING

The undersigned certify that they have read, and recommended to the Institute of Engineering for acceptance, a thesis entitled "**Fabrication of Metal Oxide/ Activated Carbon Nanocomposite from Jujube (Ziziphus Mauritiana) Seeds for Photodegradation of Dye** " submitted by Anshu Kumari in partial fulfillment of the requirements for the degree of Master in Material Science and Engineering.

Sahira

Prof. Dr. Sahira Joshi
Supervisor
Department of Applied Sciences and Chemical Engineering
Institute of Engineering
Pulchowk Campus

Prof. Dr. Rajeshwar Man Shrestha
Supervisor
Department of Applied Sciences and Chemical Engineering
Institute of Engineering, Pulchowk Campus

Prof. Dr. Hem Raj Pant
Committee Chairperson
Department of Applied Sciences and Chemical Engineering
Institute of Engineering
Pulchowk Campus
Date:

Prof. Dr. Hem Raj Pant
External Examiner
Department of Applied Sciences and Chemical Engineering
Institute of Engineering
Pulchowk Campus

ABSTRACT

The photocatalytic degradation of dye from water using metal oxide semiconductor is the study of great interest due to its environmental and health concerns. The aim of this study is to fabricate metal oxide/activated-carbon composite using zinc oxide and copper oxide with agro-base Indian Jujube (*Ziziphus Mauritiana*) activated-carbon for dye degradation from aqueous solution. Indian Jujube seed was used to synthesize agro-based activated carbon (JAC) using $ZnCl_2$ as an activating agent at carbonization temperature 500°C for 3 hrs. Thus, prepared JAC was used to synthesize metal oxide/activated carbon nanocomposites by one-step hydrothermal process. Both, activated carbon and its composite were characterized by SEM, FTIR, XRD, and UV-Vis spectroscopy. The UV-Vis spectroscopy result showed the increment in band gap of CuO in case of CuO/JAC nanocomposite from~2.3 eV to~2.6 eV while decrease in band gap of ZnO in case of ZnO/JAC nano-composite from 3.3 eV to 3.2 eV revealing the enhanced photocatalytic activity of nanocomposites. The kinetic study followed pseudo-first order kinetics for the degradation of MB & MO dye. The rate constant for MB and MO dye degradation using ZnO/JAC were 0.163 min^{-1} and 0.009 min^{-1} respectively. Similarly, CuO/JAC followed first-order kinetics in MB and MO dye degradation and the rate constants were 0.133 and 0.007 respectively. Furthermore, the results showed higher degradation rate by metal oxides nanocomposites than there pure crystal metal oxides. Therefore, Zinc oxide/activated carbon (ZnO/JAC) and copper oxide/ activated Carbon (CuO/JAC) nano-composites can be synthesized by simple, cost effective one step hydrothermal process and can be applied for effective photo-degradation of dye from aqueous solution.

Keywords: AC; Indian jujube; ZnO/JAC nanocomposite; CuO/JAC nanocomposite; MB; MO dye.

ACKNOWLEDGEMENT

The present thesis is an outcome of the contribution and co-operation of many individuals and organizations. I am very thankful to the Department of Applied Sciences and Chemical Engineering, Pulchowk Campus; and program coordinator, Prof. Dr. Sahira Joshi for providing me an opportunity to carry out and complete this thesis. I would also like to show my immense gratitude to Prof. Dr. Hem Raj Pant, Head of the Department of Applied Sciences and Chemical Engineering as this work would not be completed without his suggestions, guidance and the support. I am especially indebted to my thesis supervisor, Prof. Dr. Sahira Joshi and Prof. Dr. Rajeshwor Man Shrestha who provided me professional guidance and taught me a great deal about scientific research.

I am equally thankful to Prof. Dr. Rinita Raj Bhandari, Head of Chemistry Department who gave the permission to use the necessary laboratory facility till the completion of the thesis work. I am also thankful to my friends of M.Sc in the Material Science and Engineering 2076 batch for helping me with their ideas and suggestions. This work would not be completed without their support. I would like to specially thank to Ms Rojina Kushu, Department of Biochemistry, KU, for her guidance in the experimental characterization. I would also indebted to Department of Biochemistry, KU for providing me an opportunity to do sample characterization in their lab. I would like to express sincere gratitude and great appreciation to all the members who directly and indirectly helped me during this period of work.

I am grateful to my parents; who always guide and support me in whatever I pursue. Last but not the least; I would like to especially thanks to Manoj Gyanwali, Sugandha Shrestha, Sujan Bhandari, Kirti Bir Rajguru, Manobin Sharma, and Sunny Shah who supported me to complete this thesis work.

TABLE OF CONTENTS

LIST OF TABLES

LIST OF FIGURES

LIST OF ACRONYMS AND ABBREVIATIONS

nm	Nanometer
m^2/g	meter square per gram
mL	Milliliter
mg	Milligram
mins	minutes
hr	hour
M	Molar
MB_N	Methylene Blue Number
I_N	Iodine Number
mg/L	milligram per liter
JAC	Indian Jujube activated-carbon
VB	Valence band
CB	Conduction Band
WHO	World Health Organization
NPs	Nanoparticles
DO	Dissolved Oxygen
COD	Chemical oxygen Demand

CHAPTER ONE: INTRODUCTION

1.1 Background

In recent years, surface and ground water contamination has become a problem due to population growth. According to the World Health Organization (WHO), about 1.2 billion people live their whole life in the water crisis (UNESCO, 2012). The rapid development in industries and urban areas has led to hazardous contamination in water resources such as organic compound pollutants, heavy metals, inorganic chemicals, and many other complex compounds. It has been reported that worldwide annually, all over industries produced about 7×10^7 tons of synthetic dyes in which dyes used by only textile industries are over 10,000 tons (Chandanshive V., 2020). The dye is considered as the primary pollutant among the hazardous contaminants due to its resistance to decomposition. Dyes are used to impart the color on different substrates and used by different industries such as textiles. Synthetic dyes are classified into different categories on the basis of their origin, structure, and applications. For example: - On the basis of their chemical structure, these dyes can be classified as cationic, anionic or neutral. These dyes are widely used in textile industries to impart the color but all of them do not tightly bind to substrate, thus these effluents are discharged into water resources without prior treatment. Due to its low biodegradability, they are present in the environment for a long period of time and also show inimical effects on the living beings and photosynthesis rate of aquatic plants. This dye effluent contains toxic chemicals which are reported to be carcinogenic, mutagenic, and showing adverse effects on human health such as cancers of the kidney, urinary bladder and liver. So, the removal of dye from water resources becomes crucial.

Ergo, various suitable physical, biological and chemical purification processes have been studied to eliminate organic pollutants from the environment. The most widely used, cost effective physical methods for dyes removal are adsorption and ion-exchange. However, these methods could not remove dyes completely during the process and led to secondary pollutants and even their small amount of presence in our environment is a matter of big concern. Furthermore, most widely used adsorbents i.e., Activated carbon (AC) are difficult to regenerate and their adsorption efficiency decreases after regeneration. Other methods are coagulation/flocculation, reverse

osmosis and ultrafiltration which are associated with high cost expenditure, and limited versatility that prevents their practicability on a large scale. Biological methods have been also utilized and proved to be an alternative for dye removal, but various dyes are deliberated to resist microbial attack. Therefore both physical and biological methods have limitations on operation scale, also none of the above methods have a way to complete remediation of dye removal.

Consequently, several chemical processes have been studied such as solvent extraction, catalytic degradation and chemical oxidation etc. for water purification. However, these are also time consuming and high cost maintenance which impedes its practicability. In recent years, nanotechnology has become a promising approach in water purification for its potential approach to degrade organic pollutants by the Advance Oxidizing Process (AOP) using nano-sized photo-catalysts. Photocatalysis is a process in which semiconducting metal oxides (such as transition metal oxides) absorb photons and undergo redox reaction and break the complex organic molecules into simple fragments.

According to studies, if any photo-catalyst is physiologically photoactive, non-toxic for living beings and chemically stable is known as an ideal photo-catalyst (Lu P.J., 2011). Currently, many studies are ongoing on development of new energy resources and technologies which can control pollution in our environment. Ongoing research is focused on materials which can use renewable sources of energy such as light to degrade pollutants by an economic, regenerative and non-toxic process. Many metal oxides such as TiO_2, ZnO, CuO, and ZrO2. CdS, MoS_2, and WO_3 as semiconductors are used to degrade pollutants.

Among various transition metal oxides, TiO_2 is widely used as a common photo-catalyst due to its bio-compatible and non-corrosive nature. However, it also has defects such as expensive production and absorption bands in the ultraviolet region. Hence, Zinc oxide is also widely used in photo-catalysis as the substitute of Titanium dioxide (Nasrollahzadeh M.S., 2018). However, Zinc oxide photo-catalytic efficiency also decreases due to swift electron-hole pair's recombination. So, it is important to impede the rapid recombination of electron-hole pairs. The studies have also reported the scrutiny of another transition metal oxide such as CuO for its narrow band gap and use as p-type semiconductor. In case of narrow band gap metal oxide semiconductors,

photo absorption bands broaden farther in the visible region. However, there are some disadvantages of these photo-catalyst materials used in advanced oxidation processes. These photo-catalysts powder are easy to agglomerate which decreases its adsorption capacity, and their rapid electron-hole recombination which limits their photo-catalytic efficiency. Therefore, different studies have researched for the enhancement of the photo-catalytic efficiency of metal-oxide semiconductors and reduction in electron-hole recombination rate. Among them, one of the successful methods is introducing activated carbon with metal oxide nanoparticles. Activated carbon is widely used due to its large specific area, high adsorption capacity, and availability of micro- and mesopores. So, photo-catalyst activated carbon composites have become the trend of study for the degradation of synthetic dye-containing waste-water (Xing B., 2016).

1.2 Dye

Dyes are chemical compounds which are used to transmit colors onto substrates. In industry mainly complex organic dyes are used due to growing demand of daily life products (Ghowsi, 2014). There are two types of dyes, natural dyes and synthetic dyes. Natural dyeing is traditional and popular. The sources of natural dyes are vegetables, plant roots, insects and minerals. Some examples of natural dyes are madder, indigo. To obtain a certain color like green, the dyeing process is done twice using a combination of other colors. Synthetic dyes are mostly used ones and are available in a great variety of colors (Green & Voelker, 2003). Dyes are chemically stable and sturdy to degradation due to its complex organic structures (Siong, 2016). Ergo, the molecular structure of dyes is essential to understand for the achievement of efficient removal of dyes from effluents. Hence, dye can be referred to as a colored molecule which absorbs a certain wavelength of light from the visible spectrum range.

1.3 Methylene Blue (MB) Dye

Methylene Blue (MB) is a synthetic dye which has a heterocyclic aromatic structure with molecular formula $C_{16}H_{18}ClN_3S$ as shown in figure 1.

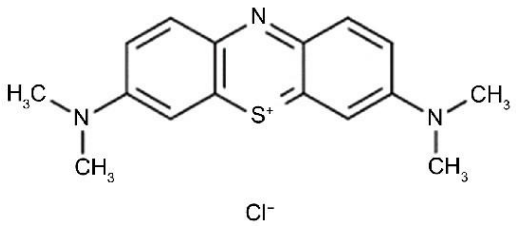

Figure 1: Molecular structure of MB (Atmani et al., 2018)

It is also known as a cationic dye, which is widely used for dying different types of fabric such as wool, silk and cotton. This dye is chemically stable and inconsistent with the base.

Uses of Methylene blue dye:

1. Industrial uses of methylene blue

   This type of dye is used in painting production, wool dyeing, other industries such as textile paper, rubber and leather etc.

2. Medical uses of methylene blue

   It is widely used for the treatment of diseases like methomoglobinemia. Due to its harmful effect, it can affect patients by increasing vascular tone and myocardial function with septic or anaphylactic shock. It is also used as cure for different diseases. Thus, controlled concentration of MB dye is also a safe drug in case of hemolytic anemia.

1.4 Methyl Orange (MO)

Methyl orange (MO) as an anionic, azo group containing dye and its IUPAC name is Dimethylaminoazobenzenesulfonate ($C_{14}H_{14}N_3NaO_3S$). It gives a bright orange color on dissolving in water and has a very high color-ability whereas persistent self-degradation. As shown in figure 2, MO contains aromatic structures and azo groups in their molecular structure. These groups are widely known for their carcinogenic and toxic nature which is harmful for our environment and bio-organisms.

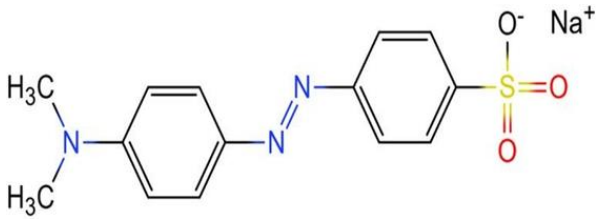

Figure 2: Molecular structure of Methyl Orange (Wu et al., 2021)

MO is also used as an acid-base indicator in research laboratories, which changes its color with a change in pH and is also extensively used in the textile industry, manufacturing of printing paper and research laboratories. Due to its resistance to degradation, if not treated efficiently it will affect human health because of the carcinogenic and mutagenic effects of dyes (Wu et al., 2021).

1.5 Dye Contaminated Water

Garment and Carpet manufacturing industry is the main source for production of dye contaminated water as their drainage line is directed directly into the river near them. Textile industries discharged a large amount of the intake water as colored wastewater due to the presence of heavy metals and organic compounds. (Kushwaha, 2014).

In the case of Kathmandu, about half of wool dyeing industries are situated near the bank of the Bagmati River (Green & Voelker, 2003). Though a number of regulations dealing with wastewater treatment from carpet industries and other industries are created, the dyes from the carpet industry still get discharged into the river. These dyes have vigorous colouring capacity which can cause problems of colour, increased Cr levels, decrease in levels of DO, and an increased level of COD in water leading to adverse effects on the environment. Dyes are chemically stable and resistive towards degradation leads to adverse effects on the environment.

1.6 Dye Removal Technologies

Water treatment methods are classified into two different categories: i) Conventional, and ii) Advanced treatment process. In conventional methods of water treatment, a sequence of operation is applied which includes removal of suspended particles, disinfection and finally chemically stabilizing the water for further use. Coagulation, flocculation, sedimentation and sand filtration are widely used to remove the suspended particles from water. However, UV light irradiation is in demand as it meets the standard protocols of disinfection. It also does not produce any by products. Moreover,

advanced technologies includes Ozonation, Ultrafiltraation, Reverse-Osmosis, Activated carbon based adsorption and advanced oxidation processes (AOPs) in water treatment (Karki, 2019). However, these water treatment processes are not efficient in the removal of synthetic dye from effluents as they only transfer contaminants from one phase to another phase and therefore lead to secondary pollution. In this context, Photocatalytic AOPs are considered as highly competitive technology as they are capable of complete elimination of non-biodegradable organic pollutants from wastewater. For the photocatalytic degradation of organic pollutants from air and water, metal oxide semiconductors have been widely used. In the photocatalytic process, the metal oxides are activated by suitable photon energy that generates the active sites of electron-hole pair. Thus, the process of degrading the adsorbed molecules in the pores of adsorbent is an interesting method to this problem.

1.7 Dye Degradation

Mateials can be classified into three categories depending on their band gap: - Conductors, Semiconductors and insulators. Those materials which have overlapped band gap despite temperature are known as conductors such as metals. The band lower than the Fermi level is known as the valence band whereas the conduction band is defined as the band above the Fermi level. In the case of a semiconductor, it possessed a gap in between these two bands. And, in the case of an insulator, it possesses a very high band gap due to which excitation of electrons from the valence band to the conduction band is difficult at room temperature. This gap is known as the forbidden band gap. However, it's easy to excite electrons from the valence band to the conduction band at room temperature due to the small band gap in the semiconductor.

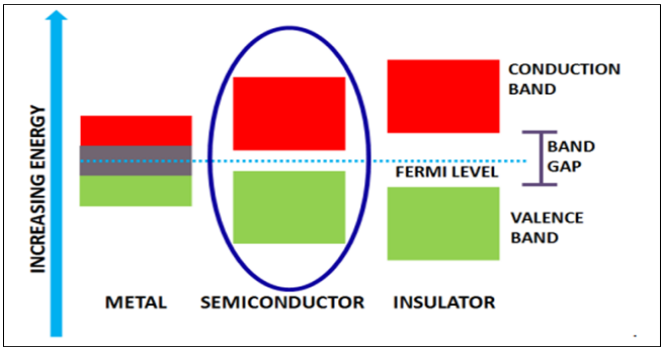

Figure 3: The structure of band gap in conductors, semiconductors and insulators (Ahuja et al., 2021)

In photocatalysis, the excitation of electrons from valence band (VB) to conduction band (CB) involves photon-energy on the surface of the catalyst. Therefore, band gap is fundamental necessary to be a photo-catalyst, which is also related to electrical and optical properties of the material. Hence, band gap engineering has become an effective approach in semiconducting materials to utilize the light energy.

In photocatalytic dye degradation, photons are absorbed (energy ≥ band gap of semiconductor) which excites electrons from valence band to conduction band and formation of holes in the VB whereas formation of electrons (e^-) in CB. Thus, e^- present in CB reduced the oxygen and generates oxide radical, whereas holes oxidize the contaminants.

Thus, holes (h^+) and electrons (e^-) act as oxidizing and reducing agents, respectively. However, the fast recombination of electron and holes reduced their photonic efficiency. Thus, the combination of porous adsorbate such as activated carbon and metal oxide semiconductors was reported as a very promising approach to reduce the recombination rate of e^- and h^+ (Ahuja, 2021).

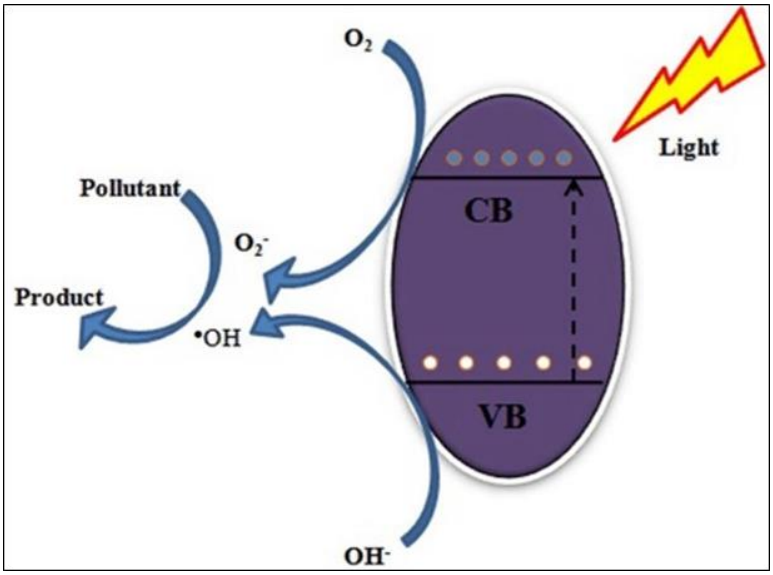

Figure 4: General mechanism of the semiconductor assisted photocatalysis (Mittal et al., 2019)

1.8 Activated-Carbon

Activated-carbon (AC) is defined as a carbon containing material with highly porous structure, and high surface area which increases its adsorption capacity (Putra Negara,

2017). These nature of AC are related to its structure and its activation method. The surface area of activated carbon varies between 500 to 1500 m^2/g (Wolf, 2014). Generally, ACs are produced from raw materials which contains low amount of inorganic materials whereas high amount of carbon such as lignite, peat, wood and coal (Hu, 2001; Pollard, 1992). The commercial production of AC is generally done by using coal which is also a non-renewable source and non-economic. Besides that, assessment of agro waste is increasing all over the world so high amount of agricultural waste materials and byproduct can be successfully converted to renewable source based AC e.g. nutshell, coconut shells, and peach stones, etc. by including two steps, namely carbonization and oxidation of the raw material (Rajbhandari et al., 2013; (Yahya, 2015).

There is the presence of different size porous structure in AC which implements the AC as widely used adsorbent and also for variety of other applications. According to IUPAC, these pores can be identified in three different groups on the basis of their dimensions (Rodriguez-Reinoso, 1985).

a. Macroporous Pores with diameters larger than 50nm
b. Mesoporous Pores with diameters between 2nm and 50nm
c. Microporous Pores with diameters (< 2nm)

1.9 Indian Jujube

Indian Jujube (*Ziziphus mauritiana*) as a precursor for preparation of AC, belonging to the family Rhamnaceae is a perennial small or medium sized subtropical tree native from Southeastern Asia, but also in various other regions such as Africa, Australia, and the Pacific It has the potential to be more widely grown as a commercial crop. In Nepal, it grows in the Terai region.

Figure 5: Indian Jujube tree with its fruits on tree and its seeds

Besides, it has significant potential as a renewable source of precursor with a unique chemical composition for the preparation of ACs with high-grades. ACs obtained from Indian jujube seeds biomass has shown high performance for adsorption of organic and inorganic pollutants for wastewater treatment, and also for supercapacitor material which would solve environmental problem such as agro-based waste disposal and pollution control (Ghimire, 2021).

1.10 Problem Statement

In present days, large number of industries produce and uses dyes such as in cosmetics, food processing, printing and textiles. This type of industries also produced colored effluents which are discharged in environment without any prior treatment and severly effects the environment. The dye materials possessed harmful effects on health such as vomiting, nausea, diarrhea, and gastritis, difficult breathing etc., (Ratna, 2015). Hence, it is important to complete degradation of these dyes from the water system. Photocatalytic degradation of dye by metal oxide nanocomposite is known as the simple, cost-effective techniques for efficient decomposition of traces of dye from water.

Recently, semiconductor photo-degradation is considered as most promising techniques which are based on the photo-degradation of harmful pollutants by photocatalytic reactions. It involves the complete degradation of organics into carbon dioxide and water rather than transferring them from one phase to another phase. The process completely oxidizes organic pollutants within a few hours, even at ppb level, without formation of secondary hazardous products. For photocatalytic materials, various metal oxides have been widely studied such as TiO_2, ZnO, CuO and Fe_2O_3 particles. It is reported that, ZnO and CuO particles doped activated carbon has ability

to degrade a large number of organic pollutants and toxic intermediates formed after the initial adsorption. Though metal oxide nanoparticles of abundantly available metals such as zinc and copper are known for degradation of dye, however rapid recoupling of electron-hole pairs and recycling of particles is major problem in dye degradation process. Furthermore, In Nepal various bio-waste materials such as rice-husk, coconut shell, sugarcane bagasse etc. have been reported for preparation of activated carbon for dye removal. In this regards, modified activated carbon from Indian Jujube seed stone with metal oxide can be economical and effective photocatalyst for dye degradation. Hence, the current study will explore the fabrication of the ZnO and CuO particles doped agro-based Indian jujube activated carbon and their kinetic study of photo-degradation of MB (cationic) and MO (anionic) dye.

CHAPTER TWO: OBJECTIVE

The objectives of this research are classified into main and specific objective which are as follow:

2.1 Main Objective

To fabricate metal oxide/activated carbon nanocomposites using zinc oxide and copper oxide with prepared activated carbon from Indian jujube (Ziziphus Mauritiana) seeds and comparative study of their photocatalytic activity.

2.2 Specific objectives are:

i. To synthesize agro-based activated carbon (AC) from Indian jujube (Ziziphus Mauritiana) seeds by chemical activation with zinc chloride.
ii. To characterize agro-based activated carbon by (Indian jujube seeds) by FTIR spectroscopy, XRD and SEM.
iii. To fabricate ZnO/AC and CuO/AC nanocomposites by hydrothermal process.
iv. To characterize synthesized activated carbon composite by FTIR spectroscopy, XRD diffraction and SEM.
v. To study the photocatalytic degradation of dye from synthetic solution using metal oxide/activated carbon nanocomposite.

2.3 Rationale

This study is focused on the fabrication of metal oxide/activated-carbon nano-composite photo-catalyst using zinc oxide and copper oxide as metal oxide with Inidian jujube seed stone activated carbon. The further study is based on their photocatalytic property of cationic and anionic dye degradation from aqueous solution. This kind of study is very important as very few academic studies have been reported regarding effect on band gap of ZnO and CuO after synthesis of metal oxide/activated carbon nano-composite. This study is also very important as it is focused on n-type (ZnO) and p-type semiconductor photocatalytic degradation property towards the cationic and anionic dye. The scientific study reported by (Shrestha, 2020) showed the high efficiency of photocatalytic degradation of MB dye using ZnO/activated carbon composite whereas it does not include the effect on band gap of zinc oxide and its recyclability. Similarly, very few study is reported about the effect on photocatalytic

dye degradation rate of cationic and anionic dye using composite of copper oxide with agro based activated carbon from Indian Jujube seed as a precursor. In the article reported by Yusoff (Yusoff, 2013), successful decoration of copper oxide on functionalized graphene sheets by a simple hydrothermal process. Similarly, the report on green synthesis of CuO nanoparticles using rhizome extract by Shrestha (Shrestha, 2022) has been shown the increase in band gap on decreasing the size of nanoparticles of copper oxide. Ergo, this study is focused to fabrication of metal oxide composites and effects on photocatalytic property of ZnO and CuO on combining with agro based activated carbon. The success to current study might extent the residing body of knowledge. However, the objective of this study is restricted to synthetic aqueous solution of dye only.

2.4 Limitations

i. Most of the techniques for characterization of the prepared materials were not available in Nepal.

ii. The complete degradation of dye from synthetic aqueous solution using metal oxide/JAC nano-composites was carried in synthetic aqueous solution not in the real water sample.

2.5 Research Methodology

The methodology followed for this study is as following:

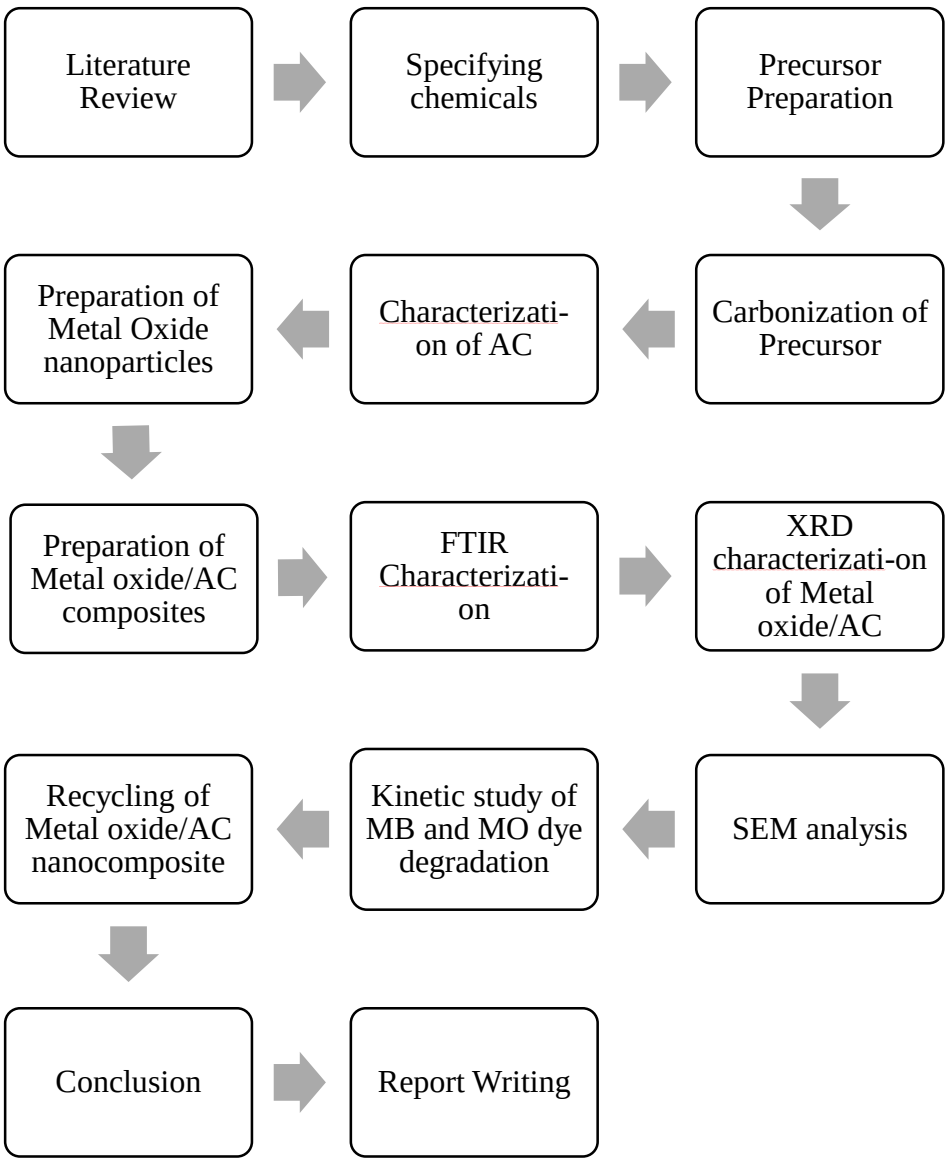

CHAPTER THREE: LITERATURE REVIEW

3.1 Research Gap

There are mainly two types of activation method for the preparation of activated carbon from the carbonaceous materials. It includes physical activation, in which raw material are carbonized at higher temperature in presence of carbon dioxide or steam. Another process is chemical activation which includes the use of chemical agents such as $ZnCl_2$, KOH, and H_3PO_4. The raw material precursor is carbonized at higher temperature with constant gas stream of N_2 after homogeneously mixing with chemical agents. Among various chemical agents for activation, $ZnCl_2$ is widely used in the preparation of ACs from various agro-waste products. Some of the reports are as follows:

Nakagawa et al., (2007) studied on activated carbon discs prepared by chemical activation of olive seed stones using H_3PO_4 and zinc chloride as an activating agent to analyze the effect on porosity of the AC. The results showed the production of large number of microporous structure by both chemicals. However, the results also showed the noticeable difference when using H_3PO_4 in case of granular and disc forms. Their study showed that zinc chloride favored the transformation of meso-porous pores into micro-porous pores of activated carbon.

Adhikari et al., (2019), prepared AC by chemical activation of walnut shells as precursor with $ZnCl_2$ (1:1 by weight) at 400°C, 500°C, and 600°C carbonization temperature for 3hrs. These studies showed that presence highly porous structure and amorphous nature of activated carbon. The ACs prepared at 400°C and 500°C showed relatively similar number of presence of micro-porous and meso-pores.

Joshi et al., (2020), reported the effect on porous structure of ACs by varying the impregnation ratio of chemical activating agent $ZnCl_2$ with precursor i.e., 0.25:1, 0.5:1, 1:1, and 2:1. This study also reports about the effect on porous structure of ACs on varying carbonization temperature which are 400°C, 500°C, and 600°C. For this study, they used sugarcane bagasse powder as precursor for AC. From the results, it was observed that increment in micro-porous structure initially, on increasing impregnation ratio up to 1:1 whereas decrease in these structure on further increasing. Similarly, the

effect of carbonization temperature showed in increment of micro-porous structure on increasing temperature from 400°C to 500°C whereas decrease on further increment in temperature from 600°C to 700°C.

Sharma et al., (2020) prepared activated-carbon (AC) by chemical activation using $ZnCl_2$ by 1:1 weight ratio with precursor at 400°C for 3 hrs. In this study, Giant Reed Cane was used as the precursor for preparation of AC and iron oxide/activated carbon composite for Arsenic removal from aqueous solution. The as synthesized AC was characterized by SEM and EDX which showed presence of different size of pore structure and amorphous nature of AC.

The above studies showed that the various agricultural wastes are used for preparing ACs using $ZnCl_2$ as an activating agent.

In recent years, dyes are enormously produced and used by many industries and effluents are released into water without any prior treatment. As these synthetic dyes are resistant to self-degradation so, these are harmful for the environment and living beings health. Thus, the development of systematic methodology to eliminate these synthetic dyes by renewable sources of energy have been become essential. Similarly, photo-catalysts have been become hot topic in present era as they interact with light. Various reports have been studied and shown the successful fabrication of metals oxide/activated carbon composite using ZnO and CuO with carbonaceous materials

.

Poulios et al., (2003) reported about the degradation of eosin Y, using TiO_2 P-25 and ZnO as photo-catalyst. The studies showed the decomposition of the organic molecule followed approximately a pseudo-first order kinetics according to the Langmuir-Hinshelwood model.

Liu et al., (2012) in this study, they processed pre-cursor via deposition-precipitation method and further by heat treatment method for preparation of g-C3N4/ZnO composite. The prepared composite were applied to study the photo-catalytic degradation of RhB & photoreduction of Cr^{+6} under visible light irradiation. In this study, prepared composite revealed higher photocatalytic properties than that of pure form of C_3N_4 or ZnO.

Yin et al., (2012) reported on the photo-catalytic properties of Ag doped Zinc oxide nanocomposite by degradation of MO from aqueous solution under irradiation of UV light. The nanocomposite was fabricated in two steps: In the first step Ag-hybridized ZnO was synthesized through a powder-sol process, then adsorption process was used to synthesize Ag/ZnO-AC composite. In the photodegradation of MO dye experimental study, Ag/ZnO-AC showed almost complete degradation whereas ZnO-AC, Ag/ZnO and pure ZnO showed 70%, 67%, and 61% degradation respectively, under UV light irradiation for 150 min. In this study, the apparent rate constant of degradation (k) for Ag/ZnO-AC and ZnO/AC was found to be $1.885 * 10^{-2}$ and $0.804 * 10^{-2}$ min^{-1} respectively.

Hongchao et.al, (2014) investigated the photocatalytic activities of the catalysts (Cu-Cu2O-CuO/ AC composites) under visible light irradiation by photocatalytic degradation of reactive brilliant blue KN-R. The result showed efficient degradation of dye using copper oxide/AC composite than pristine CuO and AC.

Arun et al., (2015) reported the characteristic study of anisotropic plate shaped CuO nanostructures by one-step and economic hydrothermal process. The preparation of CuO was confirmed by SEM, EDX, XRD, FTIR and UV/Vis/NIR spectroscopy. The spectroscopic results showed the successful formation of CuO nanoparticles. The average size of particle was 27 nm and 4.2 eV band gap which was higher than that for bulk CuO (2.1 eV).

Adhikari et al., (2015) reported the effect on photo-catalytic activity of ZnO/g-C_3N_4 nano flower structure photo-catalysts on varying the amount of graphitic carbon nitride with ZnO. In this study, nano flower structures of ZnO were synthesized by one-step hydrothermal process. These composites were characterized by different spectroscopy. The result shown that the successful growth of ZnO nano-flower structures on g-C_3N_4 sheet. The experimental study showed that the higher degradation of MB dye by 20 mg of g-C_3N_4 with ZnO composite than that of 10, 30, 40, and 50 mg of g-C_3N_4 with ZnO.

Vinayagam et al., (2016) investigated the effect on band gaps and photocatalytic degradation property of Zinc oxide/ Waste biomass activated carbon (WBAC) with different ratio 3:1, 2:2, and 1:3 respectively. The nanocomposite were synthesized by one step hydrothermal process. The result showed that the decrease in band gap as 3.17 eV, 3.04 eV, and 2.84 eV with different loading of activated carbon from 3:1, 2:2, and 1:3 in ZnO/WBAC nanocomposite respectively. The photocatalytic degradation of Orange-G dye under sun-light and UV light irradiation was investigated in which UV irradiation showed higher degradation.

Chen et al., (2017) reported about the effect on photocatalytic activity of Ag doped ZnO photo-catalysts. In this study, they used different precursor based activated carbon to prepare the composite. The experimental study on photocatalytic degradation of MO dye under visible light showed higher efficiency of coconut husk based AC with Ag-ZnO composite. The kinetic study of composite followed pseudo first-order kinetics

Mehr & Sorbiun, (2017), synthesized zinc oxide and CuO nanoparticles by a cost effective and environment friendly green synthesis process. In this study, they used ferulago angulata (schlecht) boiss extract. The XRD characterization showed that nanoparticles were synthesized in which particle size was about 44 nm. The experimental study of dye degradation was studied using RhB under Vis-light irradiation using metal oxide nanoparticles. The results showed that photocatalytic degradation performance of ZnO nanoparticles (NPs) were higher than that of CuO NPs.

Nayeri et al., (2020) reviewed several research articles related to the metal oxide modified activated carbon. They discussed the advanced and effective methods utilized for the waste-water treatment so that harmful effect on environment could be minimized. They compared the various absorbent with the respect of the removal efficiency. They also analyzed the various carbon composites in term of the operational and environmental parameters such as initial pH, absorbent dosage, and temperatures. They also discussed various kind of the applied isotherm and kinetic model.

Shrestha et al., (2020) reported on photocatalytic degradation of MB dye from aqueous solution by zinc oxide nanorod decorated on the surface of AC of agro-based lapsi (Choerospondias axillaris) seed stone precursor. The composite was synthesized by one-step hydrothermal process at 140°C for 2h. The SEM and XRD results showed adequate growth of nano-rods on the surface of AC. The experimental study of MB dye degradation under irradiation of UV light was studied. In this study, ZnO/AC composites had greater photocatalytic efficiency than other pristine catalysts.

Londono-Calderon et al., (2020) synthesized cupric oxide by simple precipitation method. The synthesized cupric oxide were characterized and used to study the oxidative decomposition of MO without using any sources of energy such as light or heat. The SEM image revealed the nanoleaf shaped structure of cupric oxide with 1.5eV indirect band gap. Thus, cupric oxide showed higher degradation towards MO dye.

Ghimire et al., (2021) studied the electrochemical performance of AC which was prepared from locally available agro-based Bayer (Ziziphus Mauritiana) with potassium hydroxide (KOH) in 1:1 ration by weight at two different temperature (500°-700°C). As synthesized activated carbon showed higher porosity and surface area at 700°C whereas its surface area at 500°C was only about 323.82 m^2/g.

Houhoune et al., (2021), studied the effect of carbonization temperature on the porous structure of activated carbon prepared from ziziphus mauritiana lam by chemical activation using phosphoric acid. The carbonization was done at three temperature: 400°C, 500°C & 600°C. The results showed higher yield and high surface area of the prepared activated carbon at 500°C

Kumari et al., (2022), reported the green synthesis of CuO/reduced graphene nano-composite for the photocatalytic treatment of water. They studied the different optimized condition for the removal of Bi^{3+} and Cd^{2+} ions from aqueous solution. They also studied photo-catalytic degradation of dye which chowed 90% decomposition of MO and 98% of EBT within about 2h.

Above studies showed that metal oxides nanoparticles (e.g. TiO_2, ZnO, CuO)/AC nano-composites prepared from agro-based activated-carbon by a simple and cost-effective hydrothermal process can effectively remove different types of dyes from aqueous solution by photocatalytic degradation.

CHAPTER FOUR: MATERIALS AND METHODS

4.1 Materials Used For Activated Carbon

Indian Jujube fruits as carbonaceous precursor for preparation of AC was collected from the Terai region, Nepal. The chemicals used for this study were of analytical grade. Distilled water was used for preparation of various solutions.

4.1.1 Instruments and apparatus

The following instruments were used in the entire experiment works.

a) Auto Clave

The metal oxide/ activated carbon composite samples were synthesized in Auto Clave by one step hydrothermal process.

b) Hotbox Oven

Auto- Clave was placed in this oven and samples were also dried in hotbox oven (Gallenkamp Registered Trade Mark Hotbox oven).

c) Vacuum Oven

Metal oxide and composite samples were dried in this oven for crystal growth (Vacuum drying oven DZF-6020).

d) Centrifuge Rotator

For supernatant solution after dye degradation, solutions were centrifuged using the instrument (Centrifuge 80-2).

e) UV-Vis Spectroscopy

The band gap energy, concentration of MB adsorption for Surface area determination and dye degradation was also measured by UV/Vis Spectrophotometer (Shimadzu UV2600i).

f) FTIR Spectroscopy: The functional group characterization of as synthesized composite were characterized by FTIR spectrophotometer (IRPrestige-21, Shimadzu, KU).

g) X-ray Diffractometer

The crystallographic characterization of as synthesized activated carbon and composite were done by XRD (NAST).

4.1.2 Preparation of reagents

a) Stock solution of methylene blue:

The stock solution of MB dye was prepared on dissolving 1g MB in 1L distilled water. Thus, the standard MB solution were prepared using stock solution as per required dilution.

b) 0.1M HCl solution:

To prepare this solution, 8.3 mL conc. HCl was taken by dropper and diluted in distilled water up-to 1000mL.

c) 0.1M NaOH solution:

To prepare this solution 1g of NaOH pellets were mixed with 250mL of distilled water.

d) 0.1N Iodine solution:

To prepare the above solution, initially 3.175g of iodine was mixed with 10% KI solution then distilled water was added up to 250mL.

e) 5% HCl:

This solution was prepared by dissolving 5 mL of conc. HCl in distilled water and diluted to 100mL.

f) 0.1M Sodium thiosulphate:

This solution was prepared by dissolving 6.2 g of sodium thiosulphate in distilled water to 250mL.

g) 1% Starch solution:

This solution was prepared by dissolving 1.0 g starch in distilled water to 100 mL, heated to boil and filtered for further use.

h) 7.5M NaOH:

To prepare above solution, 30g of NaOH was mixed in 100mL distilled water.

4.1.3 Preparation of Activated carbon (JAC)

Indian jujube seeds were crushed and made fine powder after several washing by distilled water and dried at 110°C for 6h in an electric oven. About 10 g of powder was mixed with $ZnCl_2$ in the ratio of 1:1 by weight using sufficient amount of distilled water. Then, the mixture was kept in a hot air oven at 70°C for 24 h and then the sample was transferred in a horizontal tubular furnace. The carbonization process was done under

a consistent flow of N_2 at 500°C for 3 hrs. Afterward, the pH of JAC was neutralized by repeatedly washing with distilled water. At last, the obtained wet JAC was dried at 110°*C* for further use.

4.2.1 Preparation of CuO nanoparticle and CuO/JAC nanocomposite

The sample was prepared by dissolving 0.604g $Cu(NO_3)_2.3H_2O$ and 70mg of hexamethylenetetramine in 80mL of distilled water. In the second step, 1 mL of 7.5M NaOH solution was added and kept under constant magnetic stirring for 60 minutes. In case of CuO/JAC nanocomposite, 0.025g of agro-based Indian Jujube seed stone JAC was mixed in the solution and kept on magnetic stirrer for 4 hours. The final solution was transferred inside an autoclave and kept for 3 h in an electric oven at 140°C. The synthesized sample was filtered and repeatedly washed using distilled water and ethanol. The product was dried in hot air oven for 24h at room temperature. The obtained product was further dried in hot oven at 150°C for 12h to increase the crystallinity of the photo-catalyst.

4.2.2 Preparation of ZnO nanoparticle and ZnO/JAC nanocomposite

The sample was synthesized by dissolving 0.75g $Zn(NO_3)_2.6H_2O$ in 40 mL and 0.5g of hexamethylenetetramine in 40 mL of distilled water, and separately stirred for half an hour, then mixed and again stirred for one hour. The pH of solution was maintained to 11 and again stirred for 1 hour. In case of ZnO/JAC nanocomposite, 0.025g of agro-based Indian Jujube seed stone JAC was mixed in the above solution and stirred for 4 hours. The solution was poured into a Teflon crucible and kept inside an autoclave at 150°C for 2h. The synthesized sample was filtered and repeatedly washed using distilled water and ethanol. The product was dried in hot air oven for 24h at room temperature. The obtained product was further dried in hot oven at 150°C for 12h to increase the crystallinity of the photo-catalyst.

4.3 Characterization

The surface morphology of JAC was studied by adsorption of I_2 and MB, Fourier transform infrared spectroscopy (FTIR), X-ray diffraction (XRD). The prepared metal oxide/ JAC composite under different preparation conditions were characterized by degradation of MB and MO, and UV-Vis spectroscopy.

4.3.1 Iodine number

This is the widely used parameters for characterizing activated carbon performance and is defined as the number of milligrams of iodine observed by one gram of carbon. It is a measure of micro pore content activated carbon by the adsorption of iodine from solution.

The Iodine number (I_N) was determined according to the standard method (ASTM method, 2006). In determination of the I_N, 10 mL of 5% by weight HCl was added to 1gm of AC and were allowed to boil. After cooling the solution, 10ml of 0.1N iodine solution were added. The content were shaken vigorously for 30sec and filtered. The whole of the filtrate were titrated against 0.05M sodium thiosulphate solution using starch as an indicator. The reading were noted and used for calculation of iodine using the formula given below:

Iodine number = C× conversion factor

$$\text{Conversion factor} = \frac{Eq.wt.of\ Iodine \times Normality\ of\ Iodine \times 10}{Wt.of\ activated\ Carbon\ \times Blank\ reading} \qquad (1)$$

C = Blank reading - Vol. of Hypo solution consumed after the adsorption by activated carbon. Blank reading = the volume of standard hypo solution needed to determine the prepared iodine solution strength.

4.3.2 Methylene Blue number (MB_N)

Methylene blue number (MB_N) was determined based on single point according to method (Raposo et al., 2009). In this method, 0.1gm of JACs were placed in contact with 100ml Methylene blue solution of concentration 100mg/L for 3 h at room temperature followed by homogenous shaking using electric shaker (Digital VDRL Rotator -RPM-S). The solution was thereafter filtered and the remaining concentration of methylene blue was determined by measuring the absorbance at 664 nm using a UV/Vis spectrophotometer. The process of determination of methylene blue adsorbed in mg/g (MB_N) is given below:

$$MB_N\ (mg/g) = [(C_0\text{-}C_e)\ *V]/M \qquad (2)$$

Where C_0 and C_e are initial and equilibrium concentrations of MB (mg/L) respectively, M is the mass of the adsorbent in gram and V is the volume of the solution in liter (L) and MB_N is methylene blue number.

4.3.3 Surface Area

The surface area of Activated carbon was estimated by multiple regressions method using the result of iodine and methylene blue numbers (Nunes &Guerreiro, 2011).

4.3.4 Photocatalytic degradation of dye from aqueous solution

The photocatalytic degradation of MB and MO dye in presence of metal oxide/ activated carbon composite were studied by using UV/Vis spectroscopy. For this, 60 mL of 10 mgL^{-1} of dye (MB and MO separately) and 40mg of metal oxide composite was taken in a 200 mL beaker. The solution was followed by shaking for 30 min to make a homogeneous solution at 200 rpm. UV and Visible light irradiation were done by a mercury vapor lamp and the distance between the tip of the light guide and the solution was 10 cm. After that, 5 mL of aliquot was taken from the solution at constant time-intervals and centrifuged. From the centrifuged sample, the supernatant solution of MB and MO dye were observed using a UV-visible spectrophotometer at 664 nm and 464 nm wavelength, respectively.

The degradation % (C/C_0) was evaluated using the equation is given below:

$$\left(\frac{C}{C0}\right)\% = (C0 - Ct)/C0 * 100 \qquad (3)$$

Where C_0 is initial concentration of dye (mg/L), C_t is final concentration of dye (mg/L) and C is degraded concentration of dye (mg/L) (Chen, 2009).

The kinetic study of dye degradation was carried out at an increasing interval of time from 5min to 160min after keeping the sample inside the UV chamber. The pseudo first order kinetic was calculated by using Langmuir-Hinshelwood (LH) kinetics. LH kinetics is the most commonly used kinetic expression to explain the kinetics of the heterogeneous catalytic processes. LH expression reduced to first order kinetics is given by:

$$\ln\left(\frac{C}{C0}\right) = -kt \qquad (4)$$

In which C = concentration of dye after time t (mg/L),

C_0 = initial concentration of dye (mg/L),

k = rate constant and can be evaluated from the plots of $\ln(C/C_0)$ v/s time,

t = time.

4.3.5 UV-Vis spectral study

UV-Visible spectroscopy is one of the important characterization techniques to study the synthesized nanoparticles. UV-Vis spectral study was done for band gap characterization of metal oxide composites. UV-Vis absorption spectrum were plotted using Labsolution software.

4.3.6 Optical Band Gap: This can be defined as the gap between the conduction band and valence band. This can be measured as the energy required to excite an electron from VB to CB. In case of semiconductor minimum energy is required to excite the electrons from VB to CB, thus photon could excite these electrons on the absorption of photon. Further, these band gaps are divided into two types which depends on the momentum of VB and CB. If the momentum of both band is similar than i.e., direct band gap and vice-versa (Shrestha, 2022).

This can be calculated by using Tauc's equation:

$$(\alpha h\nu)^n = A\,(h\nu - E_g) \qquad (5)$$

Where, A = Energy independent constant,

h = Planck's constant,

ν = Frequency of incident photon,

α = Absorption coefficient of material and also given as f(r)

E_g = Optical band gap,

n = index that depends upon nature of electronic transition responsible for optical absorbance

4.3.7 X-ray Diffractometer

The Debye-Scherrer equation is used to calculate the size of particles, i.e., crystalline size (D):

$$D = K\lambda/\beta \cos\theta \qquad (6)$$

Where D is the size of the particle, K is known as the Scherer's constant (K=0.94), λ is the X-ray wavelength (1.54178Å), β is full width at half maximum (FWHM) of the diffraction peak

4.3.8 FTIR Spectroscopy

This is one of the best method for identification of organic compounds in any state. In this technique infrared radiation is directed at a sample, in which sample absorb some radiation and transmits rest of the radiation. It is based on electromagnetic-wave absorption due to molecular vibrations. The molecular absorption and transmission shows a spectrum and peaks in that spectrum are the fingerprints of the compound present in sample (Thompson, 2004).

4.3.9 SEM Characterization

This is used to characterize the surface morphology of samples at atom level. This electron scanning based microscopy which scans the sample by high energy beam of electrons. The atoms present in samples interact with these electrons in which few electrons get transmitted, reflected and generation of secondary electrons. Thus, it produce different signals which reveals the surface morphology of sample (Kumar, 2013).

4.3.10 Recycling of metal oxide/activated carbon nanocomposite

The metal oxide/activated carbon nano-composites were recycled for the further MB and MO dye degradation by washing distilled water and ethanol and dried for 24 h at 80° C.

CHAPTER FIVE: RESULTS AND DISCUSSION

Agro-based JAC was prepared from Indian jujube (Ziziphus Mauritiana) seeds using $ZnCl_2$ in 1:1 ratio by weight by chemical activation. The prepared JAC was characterized by Iodine number (I_N), Methylene Blue number (MB_N), surface area, FTIR, XRD and SEM technique. The prepared JAC was fabricated with zinc oxide and copper oxide separately by a hydrothermal method to enhance the photo-catalytic activity of metal oxides. Similarly, the prepared metal oxide/JAC nano-composites were also characterized by UV-Vis, FTIR, SEM and XRD techniques. After characterization, the nano-composite photo-catalysts were applied for degradation of MB and MO dye from aqueous solution by advanced oxidation process (Photo-degradation).

5.1 Characterization of Activated Carbon (JAC):

5.1.1 Iodine number (I_N), Methylene Blue number (MB_N), and Surface Area (S.A.) analysis:

The MB_N, I_N, and S.A. of the agro-based JAC (Series1) and commercial activated carbon (series2) are presented in the Figure 6:

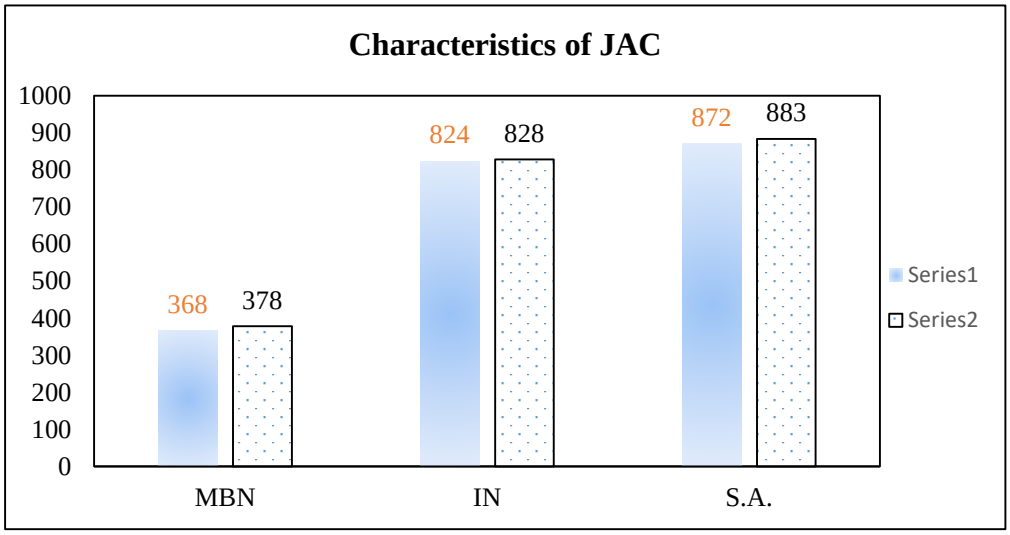

Figure 6: Results from MB_N, I_N and S.A. of the JAC

As illustrated in figure 6, I_N and surface area of the JAC is high whereas methylene blue number is low as compared to others. The MB_N, I_N, and S.A. of activated carbon are 368 mg/g, 824 mg/g and 872 m^2/g respectively. It indicates that the prepared JAC contains highly micro and meso-porous structure and high surface are and these values

were also compared with commercial activated carbon which showed similar results. The availability of these pores on the surfaces of carbons could be due to the evaporation of $ZnCl_2$ as an activating agent while carbonization. During carbonization, activating agent leaves the space which results in formation of pores. These pores can be regarded as channel to the porous systems which increases the surface area for adsorption. During chemical activation, zinc chloride acts as a dehydrating material in the process of precursor preparation from lignocellulose materials for carbonization. Analogous results were observed on the pore structure of $ZnCl_2$ as an activating agent in AC prepared from Lapsi seed stone (Rajbhandari et al., 2013; Shrestha & Joshi, 2019) with similar impregnation ratio. However, it showed better results than the pore structure of KOH activated AC at 500°C prepared from jujube seeds (Ghimire et al., 2021).

5.1.2 XRD Spectrum

XRD results helps to determine the amorphous structure of the synthesized JAC. XRD spectrum of JAC (i.e.,-AC) prepared from jujube seeds is presented in figure 7.

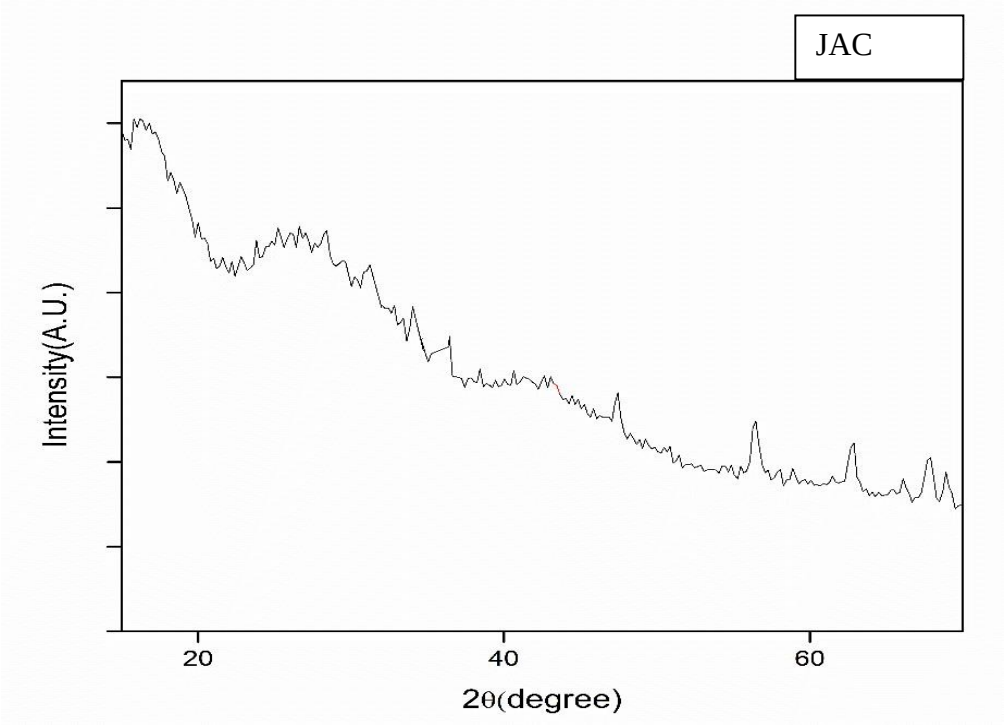

Figure 7: XRD spectrum of JAC

Above figure 7, shows that activated carbon exhibited very broad peaks and the absence of sharp peaks which showed amorphous nature of JAC. Similar results on X-ray diffraction was obtained in impregnation ratio of agro-based AC from Lapsi seed stone with H_3PO_4 activating agent and Sugarcane bagasse with $ZnCl_2$ activating agent (Rajbhandari et al., 2013; Joshi & K.C., 2020).

5.1.3 FTIR Analysis

The adsorptive properties of activated carbon can be revealed from the functional group present on its surface. As presented in the figure 8 below, it showed a broad band at around 3600-3700 cm^{-1} indicating vibration of the -OH group (kister & Roessner, 2012). The peaks around 2200 to 2400 cm^{-1} indicated the elongating vibration of hydrocarbon bond (Petrov, 2000). The broad peak around 1700 to 1900 cm^{-1} is inferred as carboxyl group elongating vibrations of -CHO, carboxyl, or ketones group. The band at around 1500 cm^{-1} is iterate as alkene elongating vibration in the aromatic structure which is normally present in carbonaceous organic compounds. The weak broad peak around 800 to 900 cm^{-1} is due to vibrations of aromatic C-H bending in aromatic ring (Plermjai et al., 2018). Ergo, the below graph indicated that JAC prepared from jujube seeds with $ZnCl_2$ as activating compound contains oxygenated functional groups such as –OH, >C=O

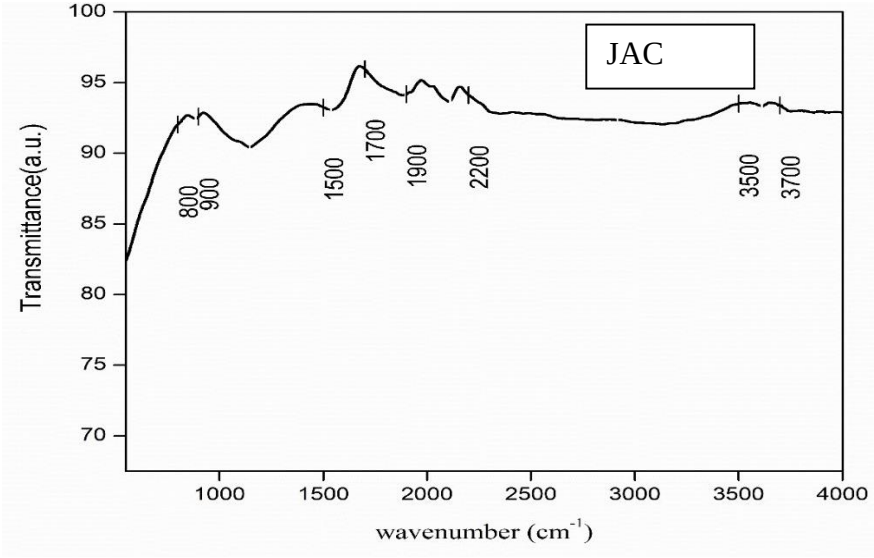

Figure 8: FTIR Spectra of Activated Carbon from jujube seeds (JAC)

5.1.4 SEM Image Analysis:

The SEM images reveal about the presence of different types of pores and impurities present on the topographical area of the materials. The porous nature of as synthesized agro-based JAC was characterized by SEM. The SEM image of JAC is shown in figure 9.

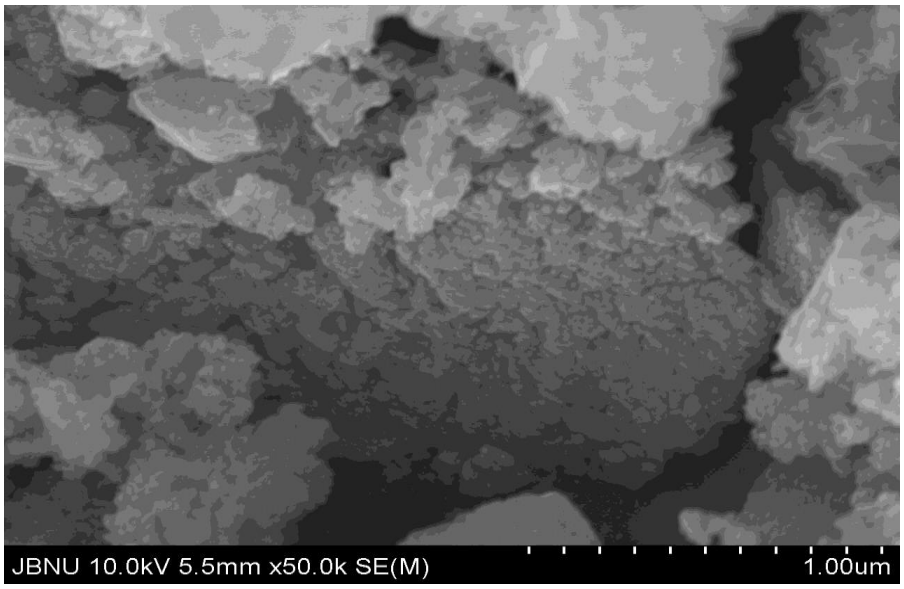

Figure 9: SEM image of agro-based JAC

As shown in above figure 9, the SEM image results showed the presence of macro-pores and meso-poroes while smidge presence of micro-pores on the surface of JAC. These pores may be formed during the chemical activation process of precursor material. The availability of pores on the surface of JAC indicates the efficient adsorptive nature of agro-based JAC prepared from Indian jujube seed stones. Thus, JAC can be used for the preparation of metal oxide/ activated carbon nano-composites.

5.2 Characterization of metal oxide/activated carbon nano-composite

5.2.1 XRD Analysis

The XRD pattern of ZnO and ZnO/JAC nano-composite is presented in figure 10:

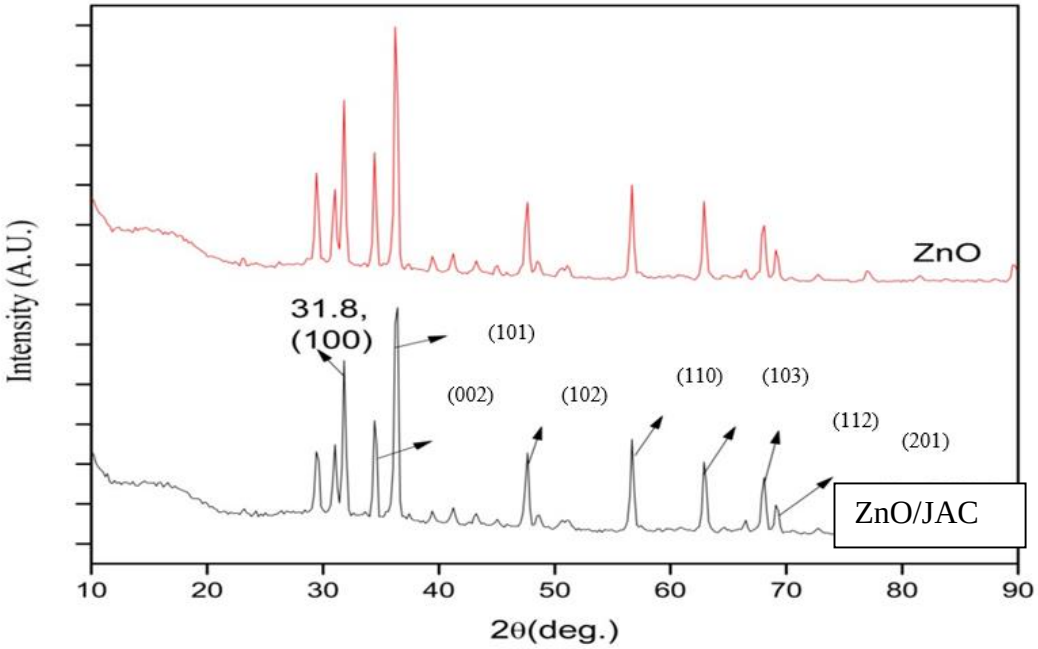

Figure 10: XRD pattern of ZnO and ZnO/JAC nano-composite

The XRD pattern of pure ZnO and ZnO/JAC nanocomposite are shown in figure 10 and the main peaks were indexed with Miller indices (h k l) which correspond to interplanar spacing of ZnO and JAC. As illustrated in figure, the sharp peaks can be observed at the 2Θ angles of 31.7, 34.4, 36.2, 47.4, 56.5, 62.8, 66.3, 67.9, 68.9, 72.5, 76.9, 81.3, and 89.5° which corresponds to the crystallites plane (1 0 0), (0 0 2), (1 0 1), (1 0 2), (1 1 0), (1 0 3), (2 0 0), (1 1 2), (2 0 1), (0 0 4), (2 0 2), (1 0 4), and (2 0 3) of ZnO respectively (ICSD-01-080-0075). This indicates the formation of pure ZnO with wurtzite structure. Furthermore, the diffraction peaks of ZnO/JAC nano-composite corresponds with the wurtzite structure of pure ZnO which confirmed the favorable growth of ZnO nano-particles on the surface of agro-based JAC. However, the existence of zenith peak of zinc oxide in case of ZnO/JAC nano-composite which might supressed the broad peak of JAC. The average crystallite size calculated was 18.36 nm for pure and 17.42 nm for ZnO/JAC nanocomposite using Debye-Scherrer equation. Analogous results of X-ray diffraction were obtained in deposition of ZnO onto the

surface of agro-based AC from Lapsi fruits (Shrestha & Jha, 2020) and graphitic carbon nitride (Adhikari et al., 2015).

5.2.2 FTIR analysis of ZnO/JAC nanocomposite

The FTIR analysis of ZnO/JAC nanocomposite is presented in figure 11:

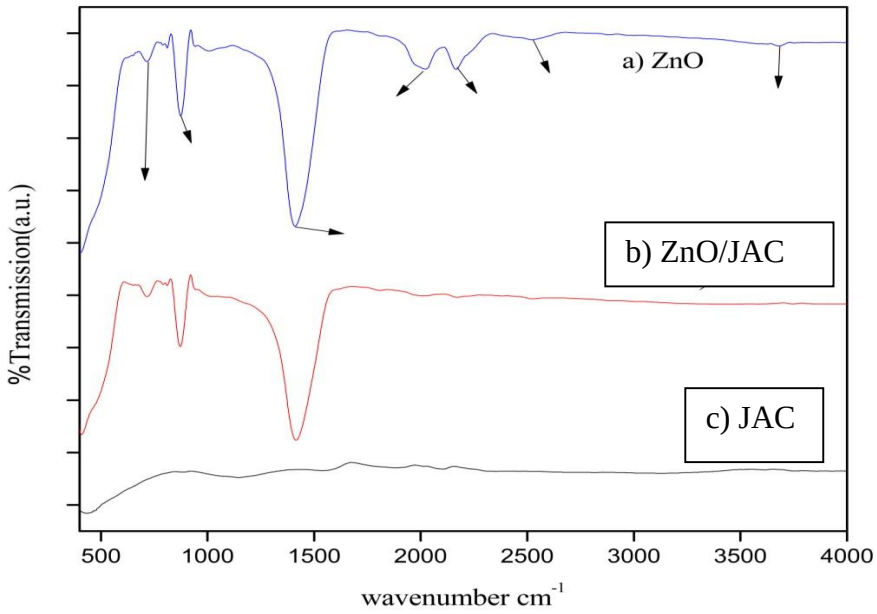

Figure 11: FTIR spectra of ZnO, ZnO/JAC nano-composite and JAC

Further FTIR characterization was done for the confirmation of formation of photo-catalyst composite and to analyze the presence of various characteristic functional group. As presented in figure 10, it iterate the presence of distinctive functional group in pure zinc oxide and zinc oxide/activated carbon photo-catalyst. The absorption peaks present at 3680 cm^{-1} described as the elongating vibrations of hydroxyl compounds. The absorption band at 2165 cm^{-1} is attributed to the vibrations of C=O bond of the carbonyl group. The peak at around 2000 cm^{-1} is attributed as the C-H bond vibrations. The peak at about 1400 cm^{-1} is attributed to the vibration of secondary alcohol. The peak at 1012 cm^{-1} inferred as the C-O bond vibration in primary alcohol or elongating vibration of the C-N bond. Furthermore, the peaks at around 500-800 cm^{-1} which is absent in activated carbon spectra iterate as elongation of the Zn-O bond.

5.2.3 FTIR analysis of CuO/JAC nanocomposite

The FTIR analysis of CuO/JAC nano-composite is presented in figure 12:

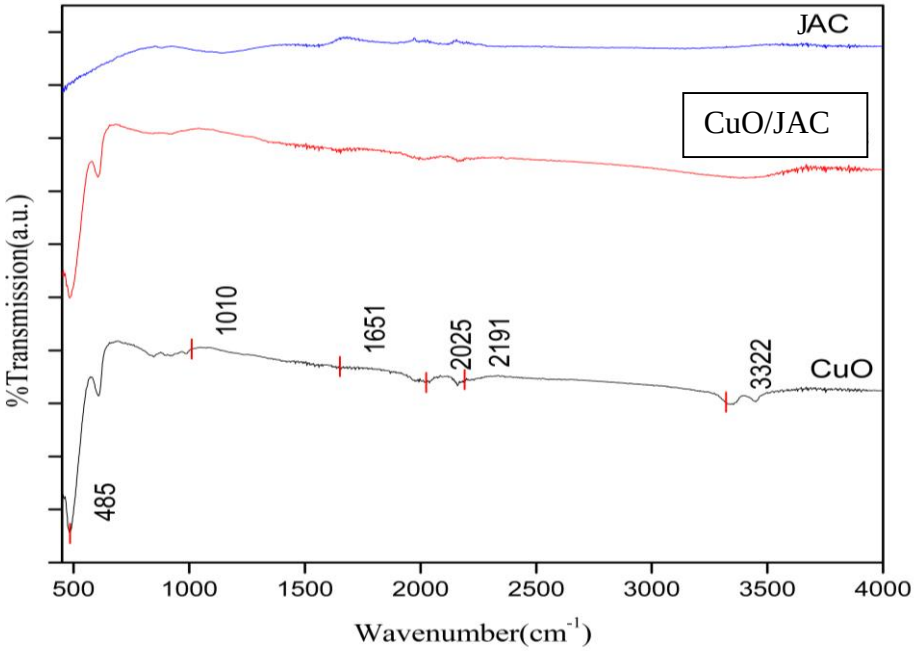

Figure 12: FTIR spectra of CuO, CuO/JAC nano-composite and JAC

As illustrated in figure 12, it indicates the characteristics functional group present in as synthesized copper oxide, copper oxide/activated carbon composite and activated carbon. The absorption peaks present at 3322 cm^{-1} inferred as the elongation vibration of hydroxyl group. The absorption band at 2191 cm^{-1} can be inferred as the C=O bond vibrations in carbonyl group. The peak at around 2025 cm^{-1} can be iterate as C-H bond hydrocarbon elongating vibrations. The peak at about 1651 cm^{-1} can be iterate as the vibration of secondary alcohol. Furthermore, the peaks at around 495 cm^{-1} which is absent in activated carbon spectra inferred to the elongating bond of the Cu-O bond hence, confirmed the formation of CuO (Shrestha et al., 2022).

5.2.4 SEM Image Analysis of Metal-oxide/activated carbon nano-composites

The SEM image of metal oxide/activated carbon agro-based Indian jujube seed stones is shown in figure 13:

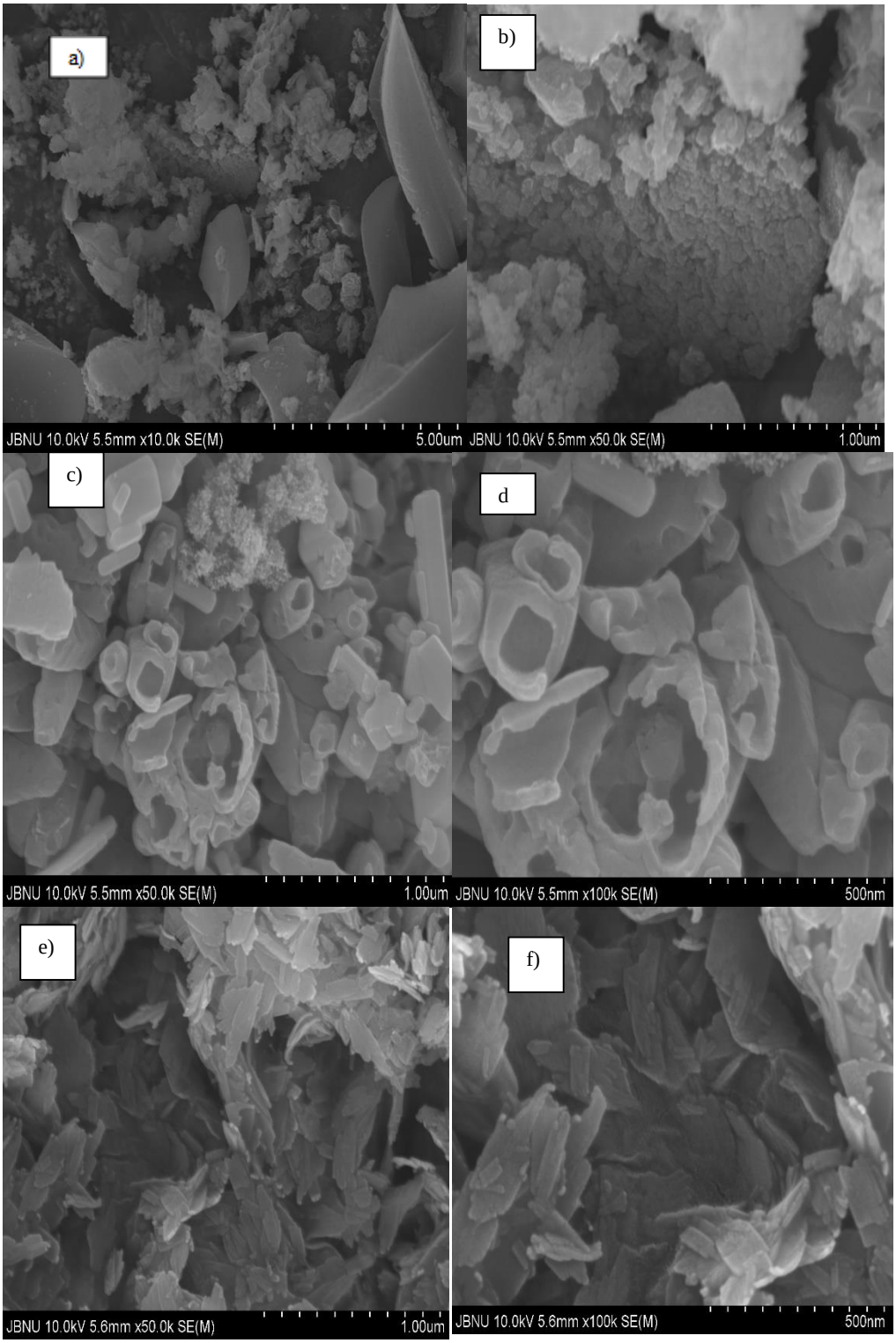

Figure 13: SEM images of synthesized samples: a) & b) JAC c) &d) ZnO/JAC nanocomposite e) & f) CuO/JAC nanocomposite

As shown in above figure 13a) &b), it revealed the smidge porous structure of agro-based AC prepared from Indian jujube seed stone which indicates the adequate adsorption nature of JAC. As indicated in figure 13c) & d), it shown the deposition of ZnO wurtzite structure nano-rods in the porous structure of JAC. Thus, the SEM image of ZnO/JAC nano-composite confirmed the successful growth and dispersion of ZnO nanorods on the surface of JAC and formation of ZnO/JAC nano-composite. It also showed immense porous structure which also includes cylindrical shape pores on the surface of composite. Analogous results were obtained from SEM image in case of zinc oxide growth on the surface of AC from agro-based Lapsi seed stone (Shrestha & Jha, 2020). Furthermore, figure 13e) and 13f) showed the dispersion of petal shaped CuO on the surface of agro-based JAC. It also ascribed the immense porous structure of CuO/JAC nano-composite which would enhance the photocatalytic activity of nano-composites. The random deposition of petal shaped CuO on the surface of JAC is inferred as the crystal growth of CuO on the surface of JAC at mild reaction parameters by hydrothermal process. Analogous results were observed from the results of SEM images preparation of copper oxide growth on functionalized graphene sheets by hydrothermal process (Yusoff & Huang, 2013). However, the SEM result showed higher dispersion of ZnO nanorods on the surface of JAC in ZnO/JAC nanocomposite than the dispersion of CuO nanopetals on the surface of CuO/JAC nanocomposite.

5.2.5 Band Gap Analysis

The band gap characterization of metal oxide/ activated carbon was characterized by UV-Vis spectroscopy. The band gap of semiconductors can determined by using Tauc Plot and Kubelka-Munk relation. The optical band gap measurement in case of photo-catalyst is an important parameter to determine the photocatalytic property. Due to the photocatallytic property, semiconductors are used in various opto-electronics devices (Jubu, 2022).Thus, the band gap of JAC, ZnO, ZnO/JAC, CuO and CuO/JAC nano-composites were evaluated by plotting the $(\alpha h\nu)^n$ v/s $h\nu$ graph. The results are presented in figure 14, 15 and 16 respectively. The result of band gap analysis by Tauc plot showed higher energy band gap in case of JAC, which can be inferred as the absence of free electrons in bands. However semiconducting nature of activated carbon can be ascribed by presence of sp^2 hybridization state of Carbon. Analogous results

were observed in enhancement of photocatalytic activity of commercial activated carbon (Velo-Gala, 2013).

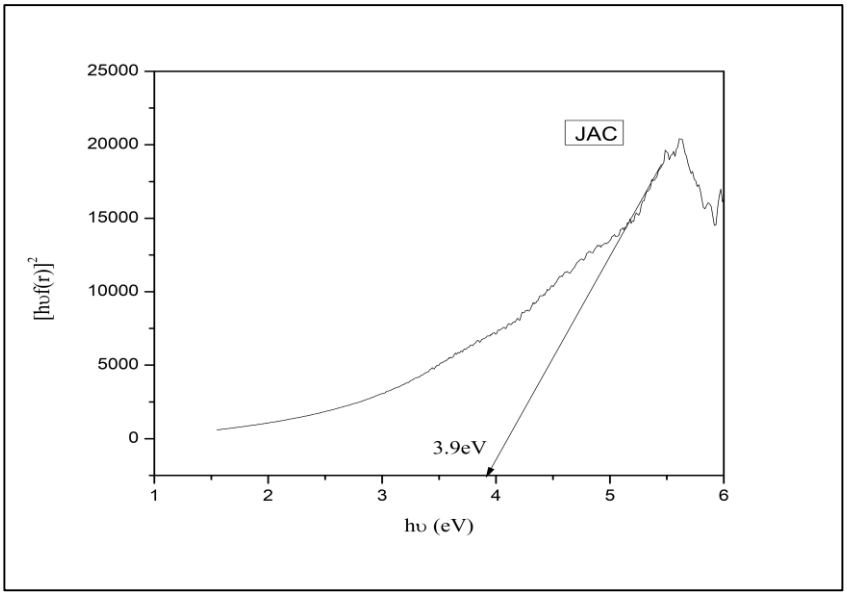

Figure 14: Absorption spectra of Indian jujube seed activated carbon (JAC)

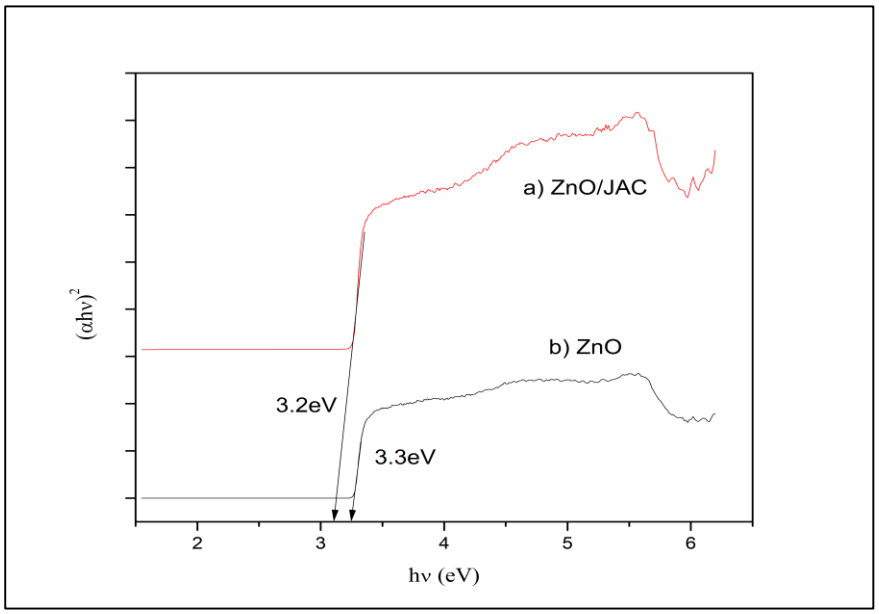

Figure 15: Effect on band gap of Zinc oxide and ZnO/JAC nanocomposite

As illustrated in figure 15, the band gap of pure ZnO and ZnO/JAC nanocomposite are 3.3 eV and 3.2 eV respectively. Thus, this showed the decrease in band gap of pure

ZnO nanocrystals on addition of activated carbon. This can be interpret as the increment of oxide radicals on the surface of the ZnO/JAC nano-composite, which lower the recombining rate of electrons from CB to holes in VB. Analogous results was observed when increasing the weight (%) of activated carbon to synthesize ZnO/AC led to decrement in band gap of ZnO/AC (Vinayagam, 2018).

Effect on Band Gap of CuO and CuO/JAC nanocomposite

The result of absorption spectra of CuO and CuO/JAC nano-composite are presented in figure 16:

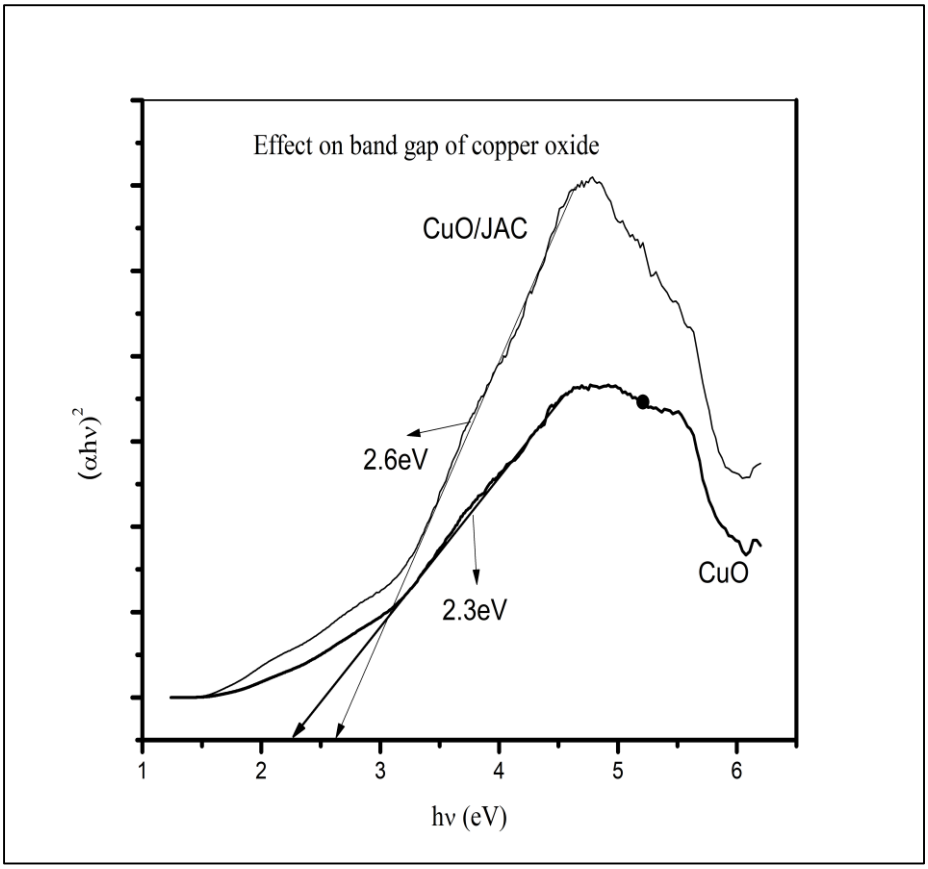

Figure 16: Band gap of CuO and CuO/JAC nanocomposite

As illustrated in figure 16, the band gap of CuO and CuO/JAC nano-composite are 2.3 eV and 2.6 eV respectively. This showed the increment in band gap energy in the case of copper oxide on the addition of activated carbon. The result of CuO band gap showed the higher band gap energy than that of bulk copper oxide (i.e., 1.5 eV), which confirmed the formation of copper oxide nanoparticles (Shrestha, 2022). Further, the increment in band gap of in case of CuO/JAC nanocomposite can be inferred as the

reduction in combination of e^- and h^+ present in CB and VB respectively. This may be due to the modification in VB and CB due to the addition of activated carbon. This can be ascribed as activated carbon acted ac charge carrier trapper which increased the band gap in CuO/JAC nanocomposite whereas decreased the band gap in case of ZnO/JAC nanocomposite (Tahir, 2021).

5.3 Photocatalytic degradation of MB and MO dye

A systematic experiments were performed to study the kinetics and degradation rate of dye concentration by photo-catalyst composites under irradiation of UV and Visible light. The recycled photo-catalyst of zinc oxide and copper oxide composite were also experimented for the decomposition of MB and MO dye under irradiation of UV and Visible light condition.

5.3.1 Photo-degradation of dye by metal oxide/activated carbon nano-composites:

The photo-catalytic activity of synthesized photo-catalysts were studied by degrading the MB as cationic dye under irradiation of UV and visible light using in a UV curing chamber. The results from UV based photo-catalytic degradation of MB and MO dye using synthesized photo-catalysts i.e., ZnO, CuO, ZnO/JAC, and CuO/JAC nanocomposite is presented in figure 17. The photo-catalytic activity of synthesized photo-catalysts were also compared with the photo-catalytic activity of commercial TiO_2-P25.

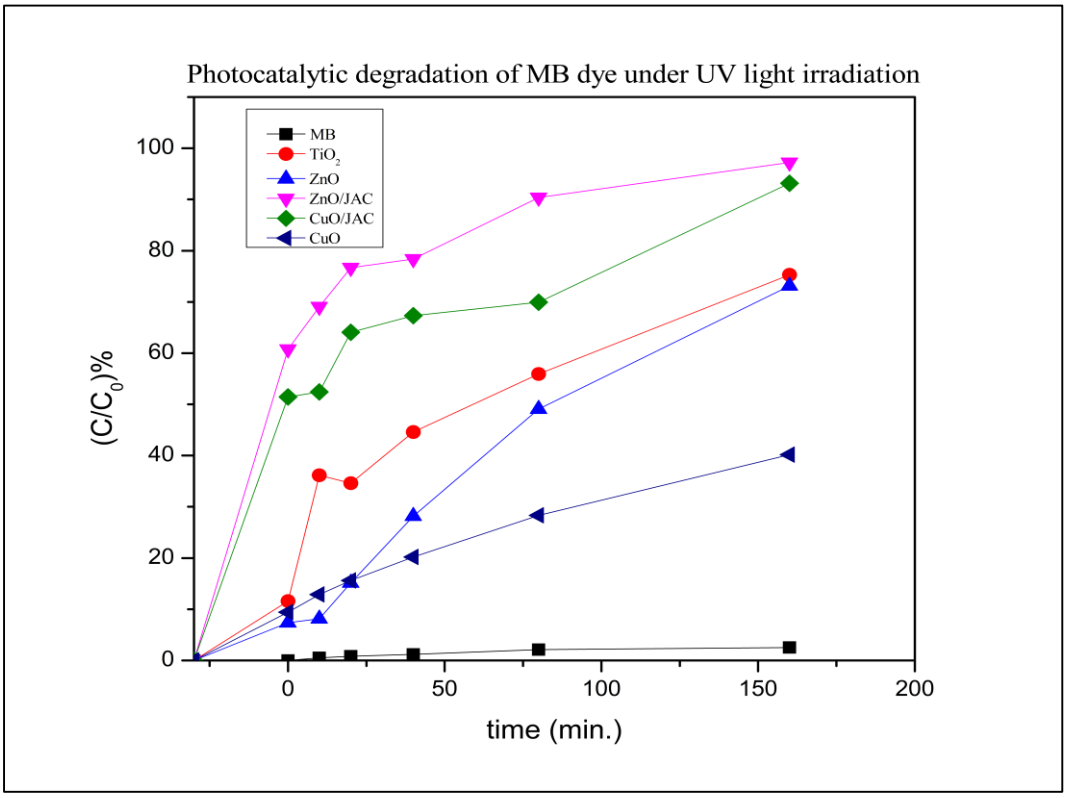

Figure 17: UV irradiated MB dye degradation (%) by fabricated photo-catalysts

As presented in figure 17, self-degradation of MB dye is negligible as these dyers are highly stable organic compounds and consists toxic nature. The result implied the higher degradation of MB dye by ZnO/JAC ~ 97.25% than other fabricated photo-catalysts whereas, dye degradation is lower in the case of CuO~47.37%. The result also revealed that fabrication of zinc oxide with JAC increased the degradation of dye than the pure ZnO ~ 74.60% crystals and commercial Titanium dioxide~ 78.32%. Similar result was also observed in the case of CuO/JAC nano-composite ~ 93.12%. On the fabrication of CuO with JAC increased its porous structure and degradation rate than the pure copper oxide crystalline particles and commercial Titanium dioxide. It can be inferred as the addition of AC with ZnO led to the decrease in recombination of e^- and h^+ pairs. Initially, the figure iterates the increasing straight line which is due to the adsorption and desorption of dye in the porous structure of photo-catalysts during shaking in dark conditions. The initial adsorption of dye on the porous surface of photo-catalysts also revealed that the porosity of metal oxide particles increased on fabrication with agro-based activated carbon from Indian Jujube seeds. Furthermore, the increased photo-catalytic activity of ZnO/JAC and CuO/JAC is inferred as the availability of electrons from the conduction-band of JAC. However, absence of electron donor from conduction-band in case of JAC, there was no change in fast recoupling of pair e^- & h^+. Analogous results were observed in the case of MB dye degradation using ZnO/AC and ZnO (Shrestha et al., 2020).

5.3.2. Effect of visible light on MB dye degradation

Similarly, MB dye degradation by synthesized phtotocatalysts were also observed under the irradiation of visible light which is presented in figure 15. The results revealed the smidge decrease in dye degradation by fabricated nanocomposites. However, ZnO/JAC~90.28% showed higher degradation than CuO/JAC~78.13%, ZnO~73.33%, and CuO~ 23.5%. Thus, it can be explained as the visible light consists higher wavelength as well the band gap of ZnO and CuO. Thus, due to the higher band gap of metal oxide nano-composites the degradation rate decreases in case of visible light. Due to the larger wavelength of light, the required energy for the excitation of electrons from valence band to the conduction band is not sufficient. Thus, it led to the decrease in degradation of organic pollutants from aqueous solution under visible light.

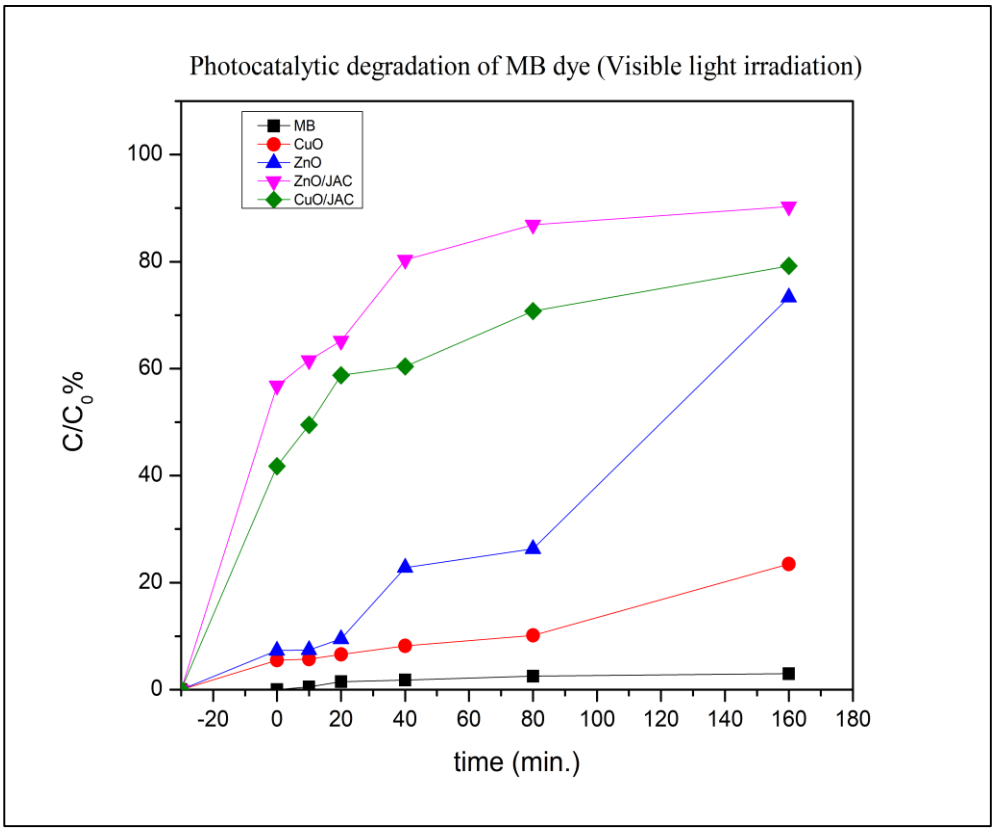

Figure 18: % Degradation v/s time graph of MB dye degradation by nanocomposites

5.3.3 Effect of UV and Visible light on MO dye degradation

The fabricated photo-catalysts were also used to degrade the MO as anionic dye under the short wavelength and longer wavelength light irradiation. The result is presented in figure 19. The degradation% in case of UV irradiation by ZnO/ JAC, CuO/JAC nanocomposites, ZnO, TiO_2-P25, and CuO are 90.87%, 90.5%, 30.7%, 25.3%, and 55% respectively. Similarly, the degradation% in case of visible light irradiation by ZnO/ JAC, CuO/JAC nanocomposites, ZnO, TiO_2-P25, and CuO are 89.4%, 86.65%, 29.3%, 48% and 28.21 %. Thus, the results revealed that huge difference between metal oxide nano-composites and pure metal oxides in case of degradation of MO dye.

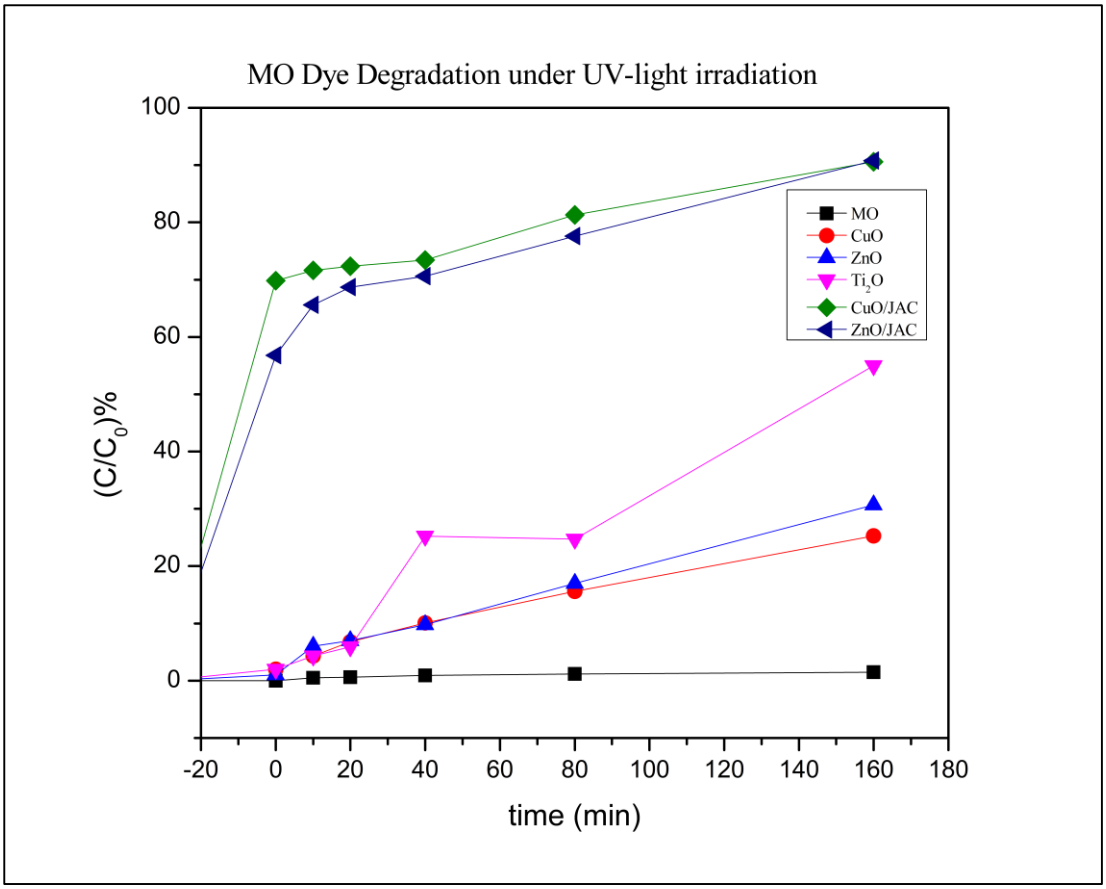

Figure 19: Effect of irradiation of UV light on % degradation of MO dye degradation by fabricated photo-catalysts

As illustrated in figure 19, MO dye did not undergo self-degradation under the irradiation by UV-light which reveals it's highly stable nature in environment. Initially, about half an hour there is smidge change in dye degradation by pure metal oxides. Therefore, it revealed the absence of porous structure on the surface of pure ZnO & CuO. It can be also inferred as the rapid combination of conduction band electrons and valence band holes. The aqueous solution of dye with photo-catalysts were shake in dark condition at constant speed. This process was done for the initial adsorption or desorption of dye on the surface of photo-catalysts. However, there is an increasing straight line in the case of ZnO/JAC and CuO/JAC for the initial 20 minutes. Thus it revealed the decrease in recombination of pair of electron and holes and porous structure of composites. However, the degradation of MO dye is lower than the MB dye. This result may be due to the difference in ionic structure and functional groups present in dyes. The MB dye consists cationic ion in its structure while MO dye consists anionic SO^{3-} functional group in its complex structure. However, in photocatalysis

hydroxyl and oxide radicals reacts with organic compounds which might hindered the degradation in case of cationic and anionic dye. Therefore, it was concluded that these radicals would interact by Coulombic forces with the cationic element of MB dye. However, metal cation (i.e., Zn^{+} and Cu^{2+}) formed during the photocatalysis would interact with anionic functional group of MO dye. Analogous results was observed in MB and MO dye elimination through photocatalysis by ZnO:Eu composite. (Trandaflovic et al., 2017).

Similarly, Irradiation by visible light on aqueous solution of MO dye was also experimented using fabricated photo-catalysts. The result is presented in figure 20.

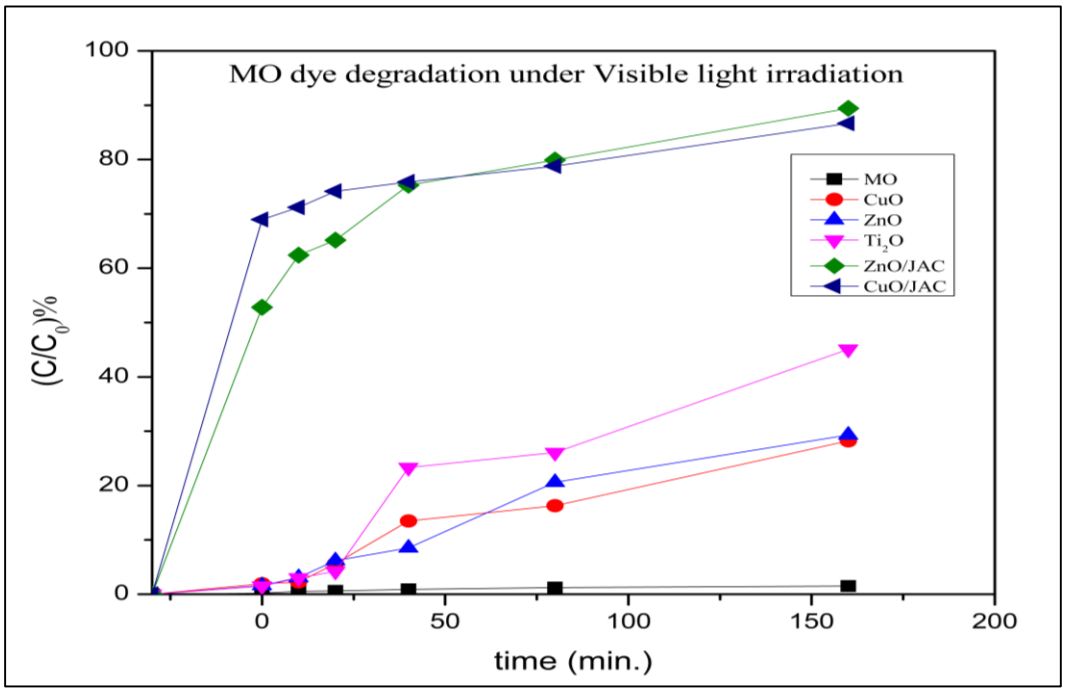

Figure 20: Effect of visible light on % degradation of MO dye by fabricated photo-catalysts

Thus, this impede the photons to reach inner layer of the catalyst. Hence, this led to decrease in excitation of catalyst particles and eventually, less e^{-} and h^{+} and hydroxyl radical were produced.

Analogous results were observed in MB dye degradation using using MWCNT/ZnO/Chitosan (Malekkiani & Magham, 2022) , and 2% Fe-ZnO composite (Isai &Shrivastave, 2019).

5.3.4 Kinetic study of applied reaction:

The kinetics models were applied in order to study the kinetics of photodegradation of MB and MO. The pseudo-first order and pseudo-second order kinetic models were used to validate the photocatalytic degradation of MB and MO dye. The first-order kinetic model is given in equation (7) (Mahmoodi, 2014):

$$\ln\left(\frac{C}{C0}\right) = -kt \qquad (7)$$

The second-order kinetic equation is given in equation (8) as per widely known expression (Mahmoodi, 2013):

$$1/C = Kt + 1/C0 \qquad (8)$$

In which C = concentration of dye after time t,

C_0 = initial concentration of dye,

k = rate constant , and can be evaluated from the plots of ln(C/C_0) v/s time for first-order, and the plots of 1/C v/s time for second-order kinetics.

t = time.

The rate constant value of photo-catalysts are given in Table 1:

Table 1: Kinetic Models of photocatalytic degradation of dye by Photo-catalysts

Dye	Catalyst	Pseudo first-order		Pseudo second-order	
		k	R^2	K	R^2
MB	ZnO/JAC	0.163	0.992	0.02	0.919
	CuO/JAC	0.133	0.965	0.008	0.9583
MO	ZnO/JAC	0.009	0.978	0.005	0.9302
	CuO/JAC	0.007	0.976	0.004	0.9339

The value of Correlation coefficient (R^2) showed in Table 1 revealed that ZnO/JAC and CuO/JAC followed pseudo first-order kinetics in MB and MO dye degradation. The ZnO/JAC nanocomposite possessed higher photodegradation rate in case of MB dye 0.163 min^{-1} compared to dye degradation by CuO/JACnano-composite i.e, 0.133 min^{-1}. However, the degradation rate decreased in case of MO dye degradation for ZnO/JAC and CuO/JAC which are 0.009 min^{-1} and 0.007 min^{-1} respectively. Thus, it was concluded that ZnO/AC and CuO/JAC nanocomposites can degrade cationic dye more faster than that of anionic dye. Analogous results was observed in photodegradation of MB and MO dye using Mn_3O_4/ZnO/Eu_2O_3 photo-catalyst. The

MB dye degradation rate constant was higher than that of MO dye degradation 0.021 min^{-1} and 0.008 min^{-1} respectively (Shubha et al., 2021). Similarly, Analogous result was observed as CuO/JAC in case of dye degradation by CuO/CNT. The result followed pseudo first-order kinetics (Mahmoodi, 2016). The results of kinetics model fitting of MB and MO dye degradation by ZnO/JAC are presented in 21 a), b), c) & d).

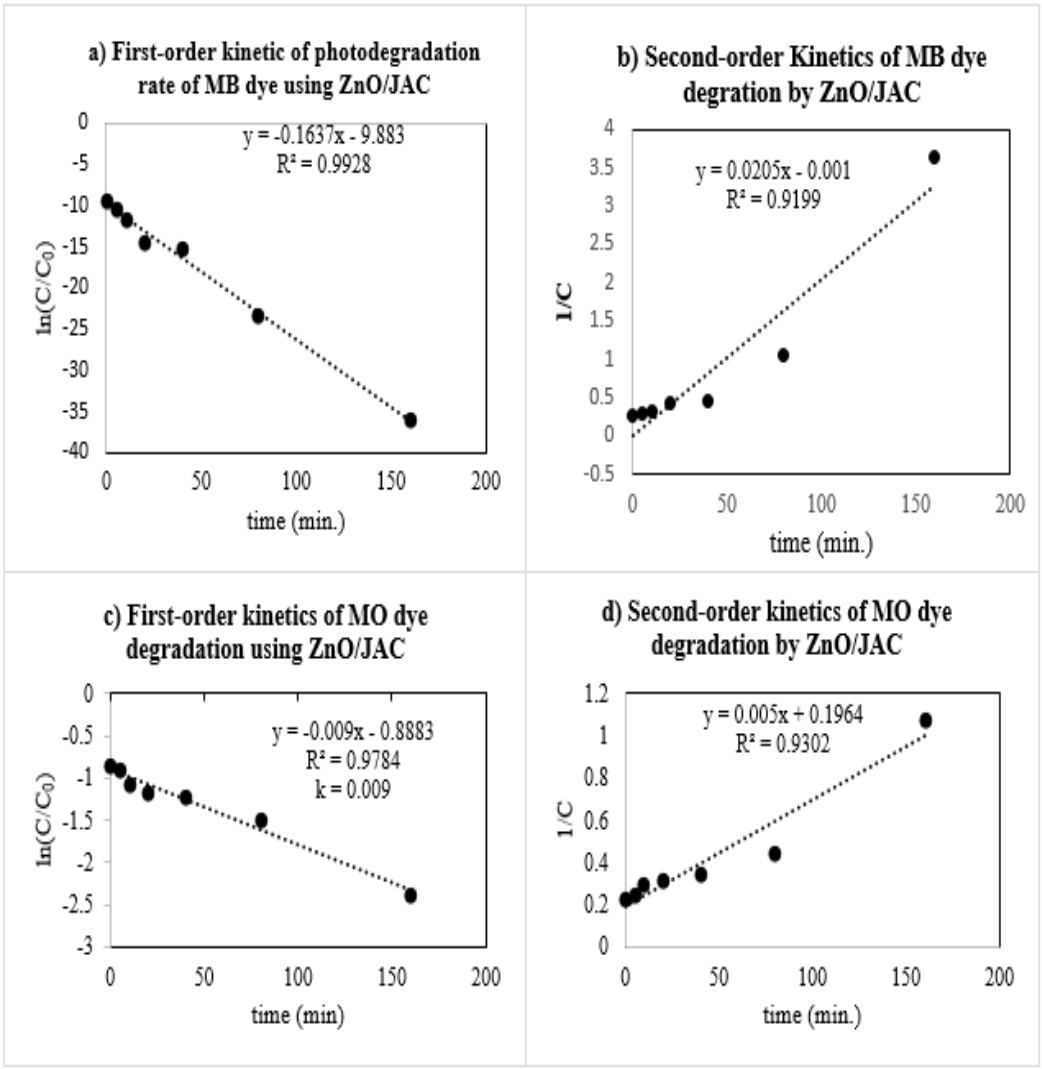

Figure 21: Kinetics analysis of MB and MO dye degradation using ZnO/JAC nano-composite

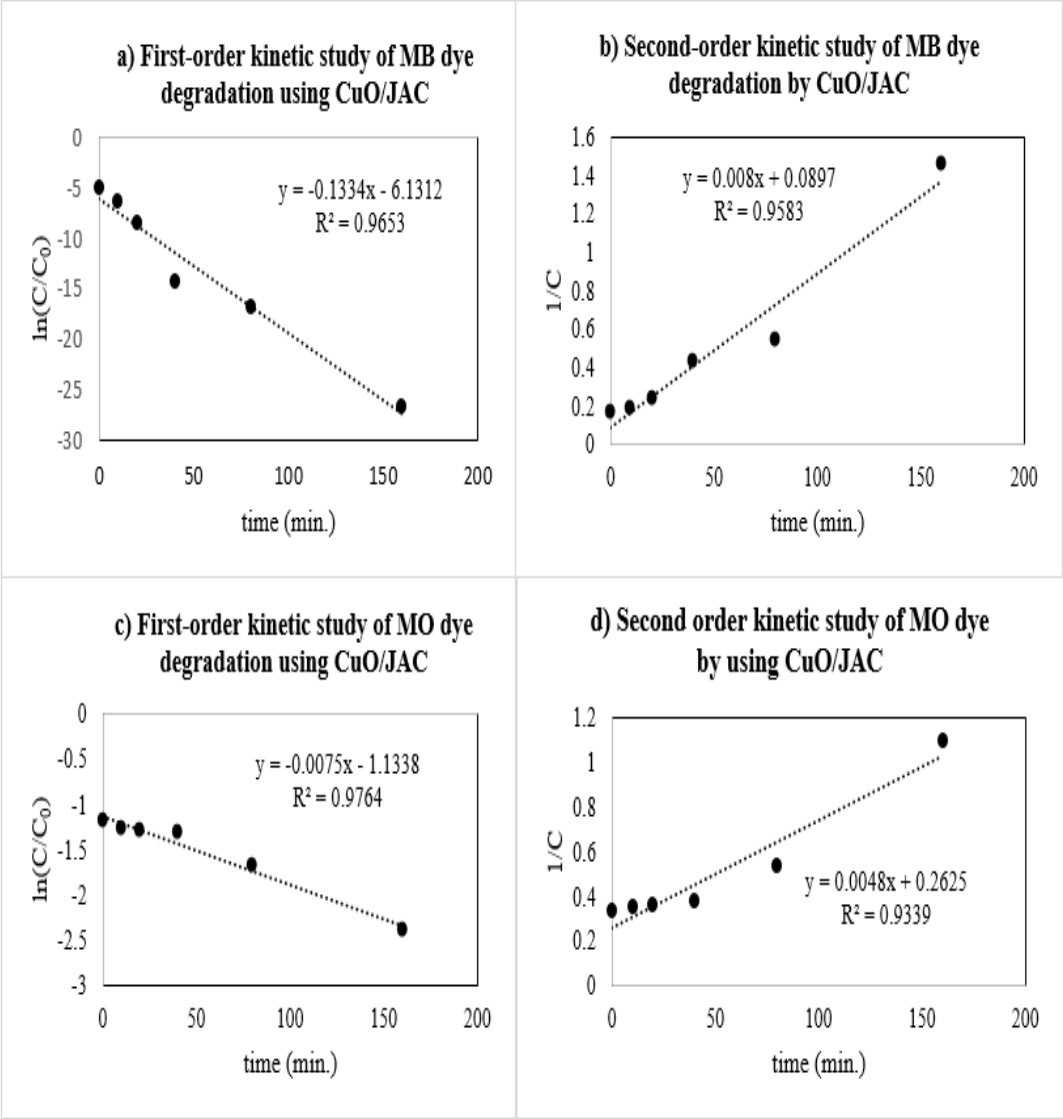

Figure 22: Kinetics analysis of MB and MO dye degradation using CuO/JAC

As illustrated in figure, it can be observed that CuO/JAC nanocomposite followed first-order kinetics in MB and MO dye photodegradation with 0.133 min^{-1} and 0.007 min^{-1} degradation rate.

5.3.5 Effect on dye degradation after recycling ZnO/JAC nano-composites

The metal oxide/activated-carbon nano-composites were recycled by washing distilled water and ethanol and dried for 24h at 80°C. The three cycles were repeated for MB and MO dye degradation by ZnO/JAC which are presented figure 23 and 24 respectively.

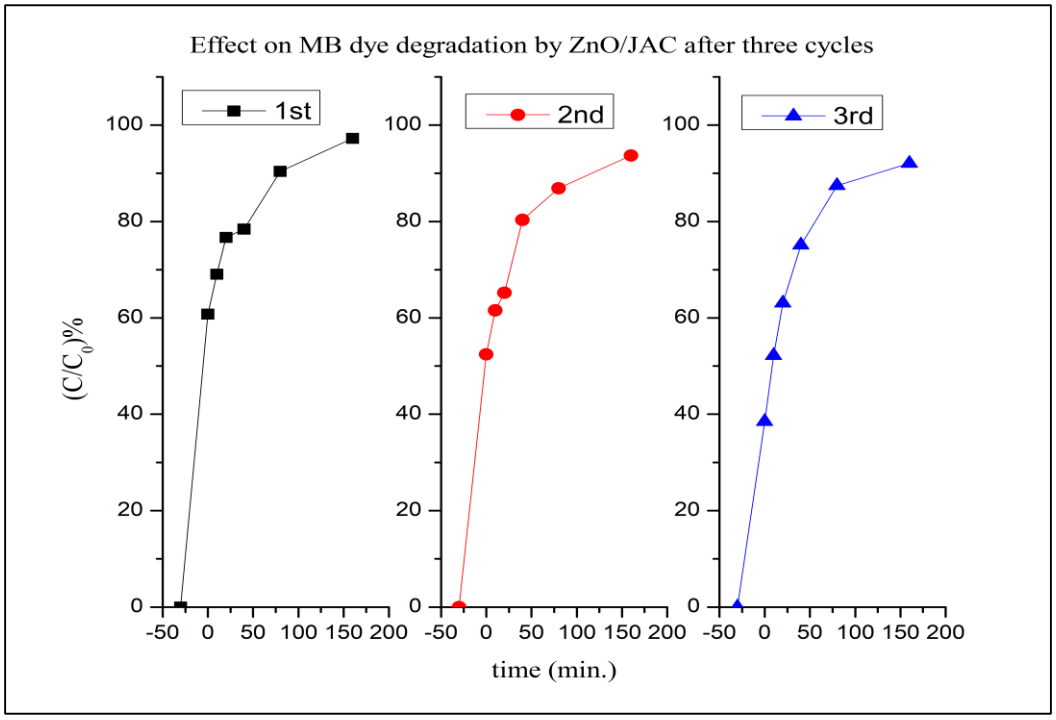

Figure 23: Effect on MB dye degradation by using recycled ZnO/JAC nanocomposite

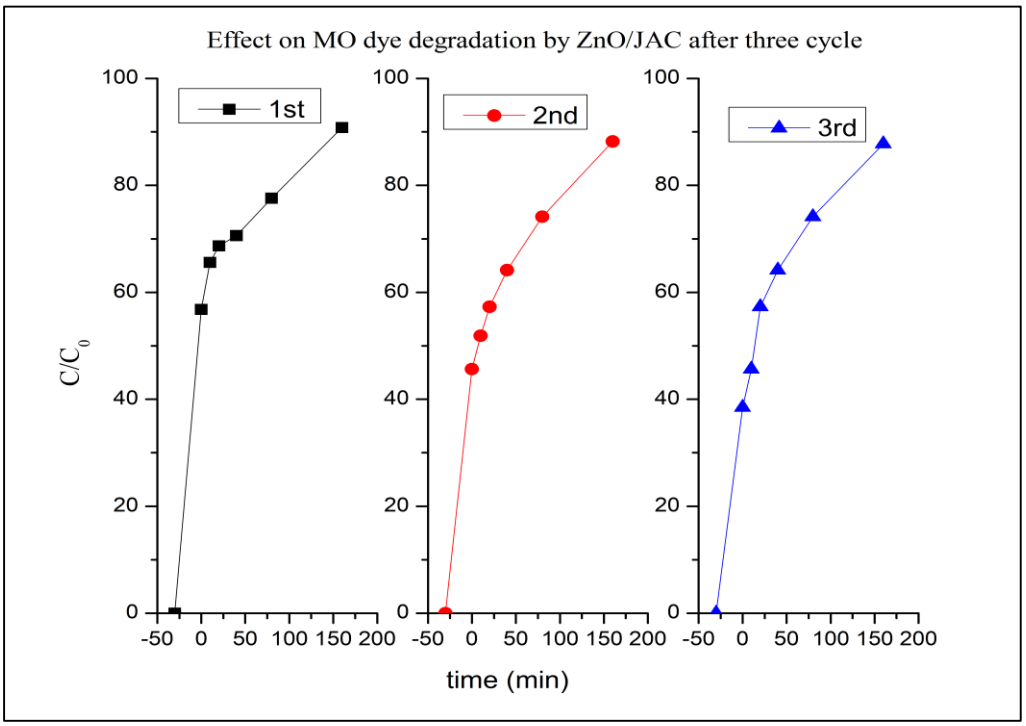

Figure 24: Effect on MO dye photo-degradation by using recycled ZnO/JAC nanocomposite

The degradation% of MB dye by ZnO/JAC in case of first, second and third recycle were 96.25%, 94.67%, and 92.08% respectively. Similarly, the degradation% of MO dye by ZnO/JAC in case of first, second, and third cycle reusability were 90.1%, 88.20%, and 85.78% respectively. As presented in figure 20 & 21, it was observed that there was negligible difference on photo-degradation of MB & MO dye even after three cycles. It showed that ZnO/AC can be reused even after a number of cycles and it would not affect the efficient degradation of organic compounds such as dye. The restoration of photo-catalytic property even after three cycles of ZnO/JAC was possible due to the fabrication of AC on ZnO. Analogous results was obtained in the case of MB-dye degradation even after three cycles of ZnO/graphitic carbon nitride sheets (Adhikari, 2015).

5.3.6 Effect on MB and MO-dye degradation on Recycling CuO/AC

The three cycles were repeated for MB and MO dye degradation by CuO/JAC which are presented figure 25 and 26 respectively.

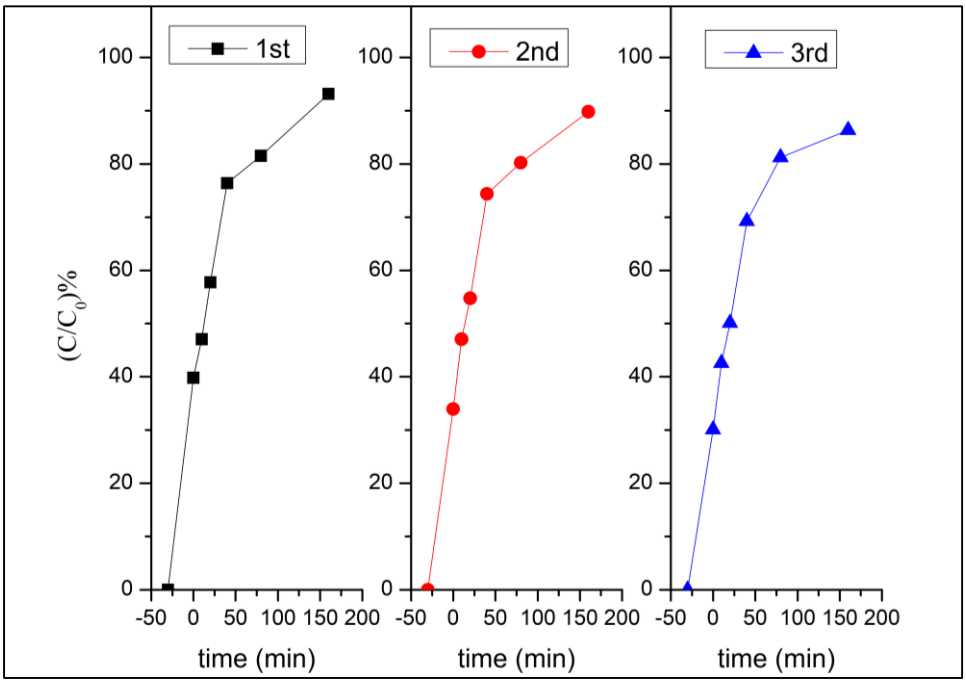

Figure 25: Effect on MB-dye photo-degradation on using recycled CuO/JAC

As presented in figure 25, the effect on MB-dye photo-degradation on using CuO/JAC showed smidge difference in third recycle than the first cycle of CuO/JAC. The degradation% of MB dye by using recycled CuO/JAC in case of first, second and third recycle were 92.47%, 92.02%, and 88.59% respectively.

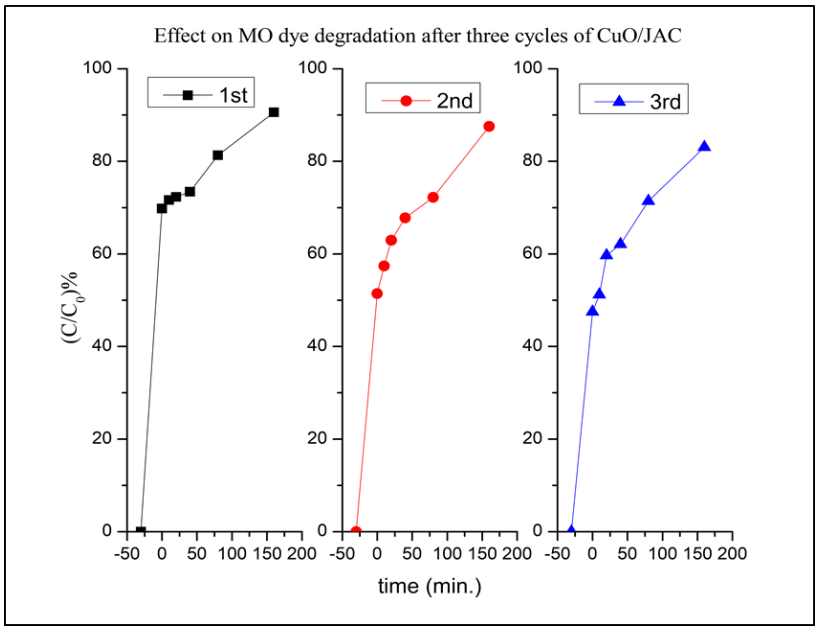

Figure 26: Effect on MB-dye photo-degradation on using recycled CuO/JAC

Similarly, the degradation (C/C_0) % of MO dye by using CuO/JAC in case of first, second, and third recycle were 90.48%, 83.56%, and 80.61% respectively. Thus, from the results, it can be inferred as fabrication of agro-based JAC with ZnO and CuO enhanced their photo-catalytic property and reusability.

The present study on dye degradation efficiency was also compared with previous research studies. The result showed good agreement with other research studies which confirmed the fabrication of zinc oxide and copper oxide on the surface of activated carbon (Table 2).

Table 2: Comparison study of photocatalytic degradation % of MB and MO dye by ZnO/AC composites

Photo-catalyst	**Light**	**Dye**	**Degrada -tion %**	**Time (min)**	**Referen-ces**
MWCNTs/ZnO/ Chitosan	UV	MB	98.76%	300	(Maghan et al., 2022)
ZnO-NR/ACF	UV	MB	99%	120	(Muna et al., 2021)
ZnO/AC	UV	MB	95%	180	(Shrestha et al., 2020)
Sn-ZnO/GO(10%)	Visible light	MO	96.2%	120	(Oyewo et al., 2022)
ZnO/AC	UV	MB	97.25%	160	Present work
ZnO/AC	UV	MO	90.8%	160	Present work

5.4 Proposed Mechanism

The proposed mechanism is summarized as follows:

- Metal oxide irradiated under UV light led the excitation of electrons from the valence band (VB) to conduction band (CB). As a result, holes (h^+) and electron (e^-) will be generated in the VB and CB respectively. The band gap is defined as the energy difference between VB and CB.
- In metal-oxides electron present in its CB are easily transferred to CB of AC due to high electric conductivity of carbon. This leads to the excitation of dye molecules adsorbed onto the Metal oxide/AC surface.
- Photoelectrons resulting from the reaction react with O_2 molecules in the solution forming ($O_2^{\cdot -}$), while holes (h^+) react with H_2O to form ($^{\cdot}OH$) that follows chain reactions.
- The ($O_2^{\cdot -}$) and ($^{\cdot}OH$) radicals react with dye molecules to convert the organic pollutants into nontoxic forms or completely decompose them to CO_2 and H_2O. Both of the photo-degradation processes are responsible for the degradation of the dye.

$$\text{Metal oxide} + h\nu \longrightarrow {}_{VB}h^+ + {}_{CB}e^-$$

$$h^+ + H_2O \longrightarrow H^+ + OH^{\bullet}$$

$$h^+ + OH^- \longrightarrow OH^{\bullet}$$

$$e^- + O_2 \longrightarrow O_2^{\bullet}$$

$$O_2^{\cdot -} + \text{organic species (dye)} \longrightarrow \text{degraded product}$$

$$OH^{\cdot} + \text{organic species (dye)} \longrightarrow \text{degraded product}$$

CHAPTER SIX: CONCLUSION

The carbonization of Indian jujube seed stone powder was done by chemical activation using $ZnCl_2$ as an activating agent. Thus presence of porous structure on the surface of agro-based AC prepared from Indian Jujube seed stones were characterized by I_N, MB_N, XRD, FTIR spectroscopy and SEM. Thus, fabrication of agro-based activated-carbon with ZnO and CuO was done by hydrothermal process. Thus, as-synthesized photocatalysts ZnO/JAC and CuO/JAC were characterized by FTIR, SEM and UV-Vis spectroscopy. The composite catalyst derived from Indian jujube seed was applied for the degradation of MB and MO dye from aqueous solution. The degradation kinetic study of MB & MO dye by ZnO/JAC and CuO/JAC nano-composite was studied. As-fabricated ZnO/JAC and CuO/JAC were recycled upto three times for the effect on reusability of nano-composites. The major conclusions are listed below:

- I_N, MB_N and surface area analysis showed that activated carbon prepared from Indian jujube seed using $ZnCl_2$ as activating agent at 500° is highly porous in nature with 824 mg/g, 368 mg/g and 872 m^2/g respectively
- XRD diffraction pattern of activated carbon showed broader peak which iterated the amorphous nature of JAC whereas the diffraction pattern of metal oxide/activated carbon showed the presence of sharp peak indicating crystalline nature.
- The results obtained from FTIR spectroscopy of synthesized activated carbon showed the existence of oxygen containing functional-groups such as C=O, -OH, -COOH and lactonic at surface of the carbon whereas metal oxide composite also showed metal oxide bonding absorption including the functional group present at the surface of activated carbon.
- The SEM images results showed the porous nature of JAC and the porosity was increased in case of ZnO/JAC and CuO/AC. It revealed the hexagonal nano-rod shape growth of ZnO in the pore structure of JAC, however nano-petals shaped growth of CuO in CuO/JAC.
- The degradation % of MB and MO dyes were higher in case of ZnO/JAC and CuO/JAC than the pure ZnO and CuO which can be inferred as the activated

carbon slowed the recombining rate of electron and hole from CB to VB in ZnO/JAC and CuO/JAC

- The degradation rate data followed pseudo first-order kinetics than second-order which indicates that ZnO/JAC and CuO/JAC can be used for complete degradation of cationic (MB) and anionic (MO) dye from aqueous solution.
- The recycling experiment showed that ZnO/JAC and CuO/JAC nanocomposite can be reused for further MB and MO dye degradation.

6.1 Recommendations

The further recommendation for the enhancement of this study are as follows:

- In present work, metal-oxide/activated carbon nanocomposites were synthesized by without varying the dose of JAC. The change in band-gap of metal-oxide/activated carbon nano-composites by varying the dose of activated carbon can be studied.
- Dye degradation was studied by using synthetic dye solution, however in further work real waste-water sample can be experimented.
- Fabrication of metal oxide/activated carbon nanocomposites can be used to study its antimicrobial or other toxic contaminants elimination from the aqueous solution.
- The electrode properties for the production of hydrogen gas by photocatalytic degradation of water can be studied.

REFERENCES

Ahmadpour, A. (1997). The preparation of activated carbon from macadamia nutshell by chemical activation. *Carbon, 35*(12), 1723-1732.

Arun, K.J., Batra, A.K., Krishna, A., Bhat, K., Aggarwal, M.D., Francis, J.P. (2015). Surfactant free hydrothermal synthesis of copper oxide nanoparticles, *American Journal of Materials Science, 5*(3A), 36-38

Aygün, A. Y.-K. (2003). Production of granular activated carbon from fruit stones and nutshells and evaluation of their physical, chemical and adsorption properties. *Microporous and mesoporous materials, 66*(2-3), 189-195.

Adhikari, S.P., Pant, H.R., Kim, H.J., Park, C.H., Kim, C.S. (2015). Deposition of ZnO flowers on the surface of g-C_3N_4 sheets via hydrothermal process. *Ceramics International, http://dx.doi.org/10.1016/j.ceramint.2015.06.134*

Bagheri, S. J. (2016). Effect of hybridization on the value-added activated carbon materials. *International Journal of Indian Chemistry,* 249-264.

Bodzek, M. &. (2012). Photocatalysis in the treatment and disinfection of water. *Ecological chemistry and engineering, S* (19(4)), 489-512.

Caturla, F. M.-S.-R. (1991). Preparation of activated carbon by chemical activation with ZnCl2, *Carbon, 29*(7), 999-1007.

Chandanshive V., K. S. (2020). In situ textile wastewater treatment in high rate transpiration system furrrows planted with aquatic macrophytes and floating phytobeds. *Chemosphere, 252*, 126513.

Chen, X., Wu, Z., Gao, Z., & Ye., B. (2017). Effect of different activated carbon as carrier on the photocatalytic activity of Ag-N-ZnO photocatalyst for methyl orange degradation under visible light irradiation. *Nanomaterials, 7*(9), 258

Deopura B.L., P. N. (2015). Chapter 5: Synthetic textile fibers: Polyamide, polyester and aramid fibers, In Sinclair, R. (Ed.), Textiles and Fashion. *Elsevier Science*.

Do M.H., P. N. (2011). Activated carbon/Fe3O4 nanoparticle composite: fabrication, methyl orange removal and regenration by hydrogen peroxide. *Chemosphere,* (85), 1269-1276.

Gao, R.J., Ding, T., Duan, X.J. (2016). Kinetics study on photocatalytic degradation of methyl orange catalyzed by sea urchin-like cuprous oxide, *Journals of Materials Science and Chemical Engineering, 4*(6), 35-40

Ghimire, J., Jha, M.K., Shah, D., Pant, H.R., Joshi, S. (2021). Synthesis and characterization of activated carbon from bayer (ziziphus mauritiana) seeds and its possibility in energy storage application. *IOE graduate conference, 9,* 2350-8906.

Ghowsi, K. E.-B. (2014). Synthesize of Zno/NPs and investigation of its effect in reduction of elctrochemical charge transfer resistance: application of it for photodecomposition of calcon (C.I. 15705) dye in various media. *International Journal of Electrochemical Science,* (9(4)), 1738-1746.

Gómez-Pastora, J. D. (2017). Review and Perspectives on the use of magnetic nanophoto-catalysts (MNOCs) in water treatment. *Chemical engineering, 301(2),* 402-427.

H., P. (2019). Fixed-bed column adsorption study: a comprehensive review. *Applied water science,* (34), 9-45.

Hongchao M., Y. L. (2014). Hongchao M., Yifeng L., Yinghuan F., Chunling Y., Xiaoli D., Xiufang Z., Improved photocatalytic activity of copper heterostructure composites (CuCu2O-CuO/AC) prepared by simple carbothermal reduction. *Australian Journal,* 749.

Houhune, M., Ouakkaf, A., Chelgham, F., Cherbi, R., Chelgam, M., Abdallah, Z.B.. (2021) Activated carbons derived by phosphoric acid activation of agricultural waste and their adsorption of methylene blue. *Asian Journal of Research in Chemistry, 14*(6).

Hu, Z. S. (2001). Novel activation process for preparing highly microporous and mesoporous activated carbons. *Carbon,* (39(6)), 877-886.

J.A. Byrne, P. D.-I. (2015). A review of heterogeneous photocatalysis for water and surface disinfection. *Molecules,* (20), 5574- 5615.

J.D. Gomez-Pastora. (2017). Synthesize of ZnO/NPs and investigation of its effect in reduction of electrochemical charge transfer resistance: application of it for photodecomposition of calcon dye in various media.

Joshi, S., Joshi, P. (2022). Removal of methylene blue dye from water using activated carbon from areca nut.

Joshi, S., K.C., B. (2020). Synthesis and characterization of sugaracane bagasse based activated carbo: effect of impregnation ratio of $ZnCl_2$. *Journal of Nepal Chemical Society, 41*(1), 74-79.

Karki, B. P. (2-19). Facile Synthesis of Magnetic Activated Carbon Composite for Arsenic Adsorption. *Journal of the Institute of Engineering,* (15(2)), 71-78.

Konnerth, P. J. (2020). Metal oxide-doped activated carbons from bakery waste and coffee grounds for application in supercapacitor. *Mater. Sci. Energy Technol.*, 69-80.

Kumar, T.S.S. (2013) Physical and chemical characterijation of biomaterials. *Characterization of Biomaterials*, 11-47

Kumar S., P. C. (2020). Performance of acid-activated water caltrop (Trapa natans) shell in fixed bed column for hexavalent chromium removal from simulated wastewater. *Environmental Science and Pollutant Research, 27*, 28042-28052.

Kumari, V., Kaushal, S., & Singh, P.P. (2022). Green synthesis of a CuO/rGO nanocomposite using a Terminalia arjuna bark extract and its catalytic activity for the purification of water. *Material Advances, 3*, 2170.

Kushwaha, A. G. (2014). Removal of caationic methylene blue and malachite green dyes from aqueous solution by waste materials of Daucus carota. *Journal of Saudi Chemical Society* (18(3)), 200-207.

Londono-Calderon, C.L., Manchaca-Nal, S., Francois, N.J., Pampillo, L.G., & Froimowics, P. (2020). Cupric oxide nanoleaves for the oxidative degradation of methyl orange without heating or light. *ACS Applied Nano Materials, 3*(3), 2987-2996. DOI: 10.1021/acsanm.0c00283.

Lu P.J., L. H. (2011). Chemical regenration of activated carbon used for dye adsorption. *Journal of the Taiwan Institue of chemical engineers,* (42(2)), 305-311.

Moradi, S. (2016). Low cost metal oxide activated carbon prepared and modified by microwave heating method for hydrogen storage. *Korean J. Chem. Eng.*

Maghan, A.H.J., Ravari, F., Dadmehr, M., Malekkiani, M. (2022). Facile fabrication of ternary MWCNTs/ZnO/Chitosan nanocomposite for enhanced photocatalytic degradation of methylene blue and antibacterial activity.

Mahmoodi, N.M, Rezaei, P., Ghotbei, C., & Kazemeini, M. (2016). Copper oxide-carbon nanotube (CuO/CNT) nanocomposite: Synthesis and photocatalytic dye degradation from colored textile wastewater. *Fibers and Polymers, 17*(11), 1842-1848.

Muna, A.D., Borhan, A. (2021). Photocatalytic degradation of methylene blue using zinc oxide nanorods grown on activated carbon fibers.

Nakagawa, Y. S.-R. (2007). Modification of the porous structure along the preparation of activated carbon monoliths with H_3PO_4 and $ZnCl_2$, *Microporous and Mesoporous Materials, 103*, 29.

Nasrollahzadeh M.S. (2018). Synthesis of ZnO nanostructure using activated caebon for photocatalytic degradation of methyl orange from aqueous solutions. *Applied water Science* (8), 104.

Nayeri, D. M. (202). Dye removal from water and wastewater by nanosized metal oxides - modified activated carbon: a review on recent researchers. *Journal of Environmental Health Science and Engineering*.

Nguyen C.H., T. M. (2019). Enhanced remediation form aqueous solutions by UV and simulated solar photocatalysis over TiO2 composites. *Separation and Purification Technology*, 115962.

Nunes, C. &. (2011). Estimation of surface area and pore volume of activated carbon by methylene blue and iodine numbers. *Quimica Nova, 34*(3), 472-476.

Parmar S., D. S. (2022). Microorganisms: an ecofriendly tool for waste management and environmental safety. *Development in wastewater treatment*, 175-193.

Pavan, F. A. (2008). Removal of methylene blue dye from aqueous solutions by adsorption using yellow passion fruit peel as adsorbent. *Bioresource Technology, 99*(8), 3162-3165.

Pollard, S. J. (1992). Low-cost adsorbents for waste and wastewater treatment: a review. *Science of the Total Environment* (116(1-2)), 31-52.

Ptasinska, S., Dramicanin, M.D., Trandafilovic, L., V., Jovanovic, D., J. (2017). Enhanced photocatalytic degradation of methylene blue and methyl orange by ZnO:Eu nanoparticles

Putra Negara, D. T. (2017). Chemical, strength and microstructures characterization of Balinese bamboos as activated carbon source for adsorbed natural gas application. *IOP Conference Series: Materials Science and Engineering.*

Rajbhandari, R. S. (2013). Development of nanoporous structure in carbons by chemical activation with zinc chloride. *Journal of Nanoscience and Nanotechnology* (13(4)), 2613-2623.

Ratna, &. B. (2015). Pollution due to synthetic dyes toxicity & carcinogenicity studies and remediation. *Geotechnique*(29(1)), 47-65.

Seok, D. J. (2019). Recent progress of electrochemical energy devices: Metal-oxide carbon nanocomposites as materials for next-generation chemical storage for renewable energy. *Sustain*.

Shrestha P., Jha, M.K., Ghimire, J., Koirala, A.R., Shrestha, R.M., Sharma, R.K., Pant, B., & Pant, H.R. (2020). Decoration of zinc oxide nanorods into the surface of activated carbon obtained from agricultural waste for effective removal of methylene blue dye. *Materials, 13,* 5667.

Shrestha, S., Shrestha, G. (2022). Biogenic synthesis of copper oxide nanoparticles using aqueous rhizome extract of rubus ellipticus for photocatalytic degradation of methylene blue.

Tahir, D., IIyas, S., Rahmat, R., Heryanto H., Fahri, A. (2021). Enhanced Visible-light absorption of Fe_2CO_3 covered by activated carbon for multifunctional purposes: tuning the structural, electronic, optical, and magnetic properties. *ACS Omega,6,42,* 28334-28346.

Thomas, C. T. (2021). Photocatalytic Treatment of Biological Organisms in Water Using Graphene Oxide Doped TiO2 and BiVO4 nanocomposites. LE MANS UNIVERSITE.

Velo-Gala, I., Lopez-Penalver, J.J., Sacnchez-Polo, M., Rivera-Utrilla, J. (2013). Activated carbon as photocatalyst of reactions in aqueous phase. *Applied Catalysts B: Environmental,* 142-143.

Vinayagam, M., Ramachandram, S., Ramya, V., Sivasamy, A. (2017). Photocatalytic degradation of orange G dye using ZnO/biomass activated carbon nanocomposite. *Journal of Environmental Chemical Engineering,* 2213-3437.

WAng, Q. Z. (2019). Copper oxide/cuprous oxide/ hierarchical porous biomass-derived carbon hybrid composites for high-performance supercapacitor electrode. *Journal of Alloys Compd.*, 11031113.

Wolf, E. (2014). Applications of Graphene: An overview in applications of Graphene. *Springer Briefs in Materials*.

Xing B., S. C. (2016). Preparation of TiO2/AC composites for photocatalytic degradation of RhB under UV light irradiation. *Journal of nanomaterials*, 10.

Xu, C. a. (2006). Supercritical water synthesis and deposition of iron nanoparticles in activated carbon. *The journal of supercritical fluids*, 135-141.

Yadav, M. S. (2020). Electrochemical analysis of CuO-AC based nanocomposite for supercapacitors electrode application. *Mater. Today Proc.*, 366-374.

Yahya, M. A.-Q. (2015). Agricultural bio-wasate materials as potential sustainable precursors used for activated carbon production: A review. *Renewable and Sustainable Energy Reviews* (46), 218-235.

Yusoff, N., Huang., N.M., Muhamad, M.R., Kumar, S.V., Lim, H.N., & Harrison, I. (2013). Hydrotherma synthesis of CuO/functionalized graphene nanocomposites for dye degradation. *Materials Letters,93,* 393-396

Zhu, M. &. (2011). Review on the progress in synthesis and apllication of magnetic carbon nanocomposites. *Nanoscale, 3*(7), 2748-27.

APPENDIX